THE FASEB JOURNAL • RESEARCH • www.fasebj.org

Sphingosine kinase 1–interacting protein is a dual regulator of insulin and incretin secretion

Yanyan Liu,* Shin-ichi Harashima,* Yu Wang,* Kazuyo Suzuki,* Shinsuke Tokumoto,* Ryota Usui,* Hisato Tatsuoka,* Daisuke Tanaka,* Daisuke Yabe,* Norio Harada,* Yoshitaka Hayashi,† and Nobuya Inagaki*,[1]

*Department of Diabetes, Endocrinology and Nutrition, Graduate School of Medicine, Kyoto University, Kyoto, Japan; and †Division of Stress Adaptation and Protection, Department of Genetics, Research Institute of Environmental Medicine, Nagoya University, Nagoya, Japan

ABSTRACT: Our previous study demonstrated that sphingosine kinase 1–interacting protein (SKIP, or Sphkap) is expressed in pancreatic β-cells, and depletion of SKIP enhances glucose-stimulated insulin secretion. We find here that SKIP is also expressed in intestinal K- and L-cells and that secretion of gastric inhibitory polypeptide (GIP) and glucagon-like peptide-1 (GLP-1) as well as insulin are significantly increased, and blood glucose levels are decreased in SKIP-deficient ($SKIP^{-/-}$) mice compared with those in wild-type mice. Plasma triglyceride (Tg), LDL cholesterol, and mRNA levels of proinflammatory cytokines in adipose tissues, livers, and intestines were found to be significantly decreased in $SKIP^{-/-}$ mice. The phenotypic characteristics of $SKIP^{-/-}$ mice, including adiposity and attenuation of basal inflammation, were abolished by genetic depletion of GIP. The improvement of glucose tolerance and lipid profiles in $SKIP^{-/-}$ mice were cancelled by GLP-1 receptor antagonist exendin-(9–39) treatment. In summary, depletion of SKIP ameliorates glucose tolerance by enhancing secretion of insulin and incretins, improves lipid metabolism, and reduces basal inflammation levels. Thus, inhibition of SKIP action may emerge as a new option for treatment of type 2 diabetes mellitus with metabolic dysfunction.—Liu, Y., Harashima, S., Wang, Y., Suzuki, K., Tokumoto, S., Usui, R., Tatsuoka, H., Tanaka, D., Yabe, D., Harada, N., Hayashi, Y., Inagaki, N. Sphingosine kinase 1–interacting protein is a dual regulator of insulin and incretin secretion. FASEB J. 33, 000–000 (2019). www.fasebj.org

KEY WORDS: inflammation · lipid metabolism · obesity

Glucose-dependent insulinotropic polypeptide/gastric inhibitory polypeptide (GIP) and glucagon-like peptide-1 (GLP-1) are the 2 primary incretins secreted from intestinal K- and L-cells, respectively, in response to nutrients. One of the main physiologic roles of these hormones is to enhance glucose-stimulated insulin secretion from pancreatic β-cells (1–3). GIP also stimulates insulin-dependent glucose uptake and lipoprotein lipase activity in adipose tissues (4, 5). GLP-1 also inhibits glucagon secretion and gastric emptying and decreases food intake, thereby leading to reduction of blood glucose levels (6, 7). In addition, GLP-1 reduces remnant lipoprotein and chylomicron production by directly acting on the intestine, the brown adipose tissues and the pancreas (8–11).

Sphingosine kinase 1–interacting protein (SKIP), also referred to as Sphkap, was reported as a novel A-kinase anchoring protein that tethers the PKA regulatory subunit I (12, 13). The molecule also was identified as a sphingosine kinase 1 (Sphk1)-interacting protein that inhibited Sphk1 activity (14). Recently, we have found that SKIP is highly expressed in pancreatic β-cells but not in α-cells (15). An intraperitoneal glucose tolerance test showed that plasma blood glucose levels were decreased, and plasma insulin levels were increased in SKIP-mCherry knockin (KI) ($SKIP^{-/-}$) mice compared with those in control mice. Glucose-stimulated insulin secretion was augmented in islets isolated from $SKIP^{-/-}$ mice. The study indicated that SKIP is a novel regulator of glucose-stimulated insulin secretion (15). However, the physiologic functions of SKIP in whole-body glucose homeostasis and other metabolic changes still remain unknown.

ABBREVIATIONS: AUC, area under the curve; CT, computed tomography; $Gcg^{gfp/+}$, glucagon–green fluorescent protein knockin; GFP, green fluorescent protein; GIP, glucose-dependent insulinotropic polypeptide/gastric inhibitory polypeptide; $GIP^{gfp/+}$, gastric inhibitory polypeptide–green fluorescent protein knockin hetero; $GIP^{gfp/gfp}$, gastric inhibitory polypeptide–green fluorescent protein knockin; GLP-1, glucagon-like peptide-1; H&E, hematoxylin and eosin; HDL-Cho, HDL cholesterol; ITT, insulin tolerance test; KI, knockin; LDL-Cho, LDL cholesterol; NEFA, nonesterified fatty acid; OGTT, oral glucose tolerance test; qRT-PCR, quantitative RT-PCR; SKIP, sphingosine kinase 1–interacting protein; $SKIP^{-/-}$, sphingosine kinase 1–interacting protein deficient; Sphk1, sphingosine kinase 1; Tg, triglyceride; VLDL-Cho, VLDL cholesterol; WT, wild type

[1] Correspondence: Graduate School of Medicine, Kyoto University, 54 Kawaharacho, Shogoin, Sakyo-ku, Kyoto 606-8507, Japan. E-mail: inagaki@kuhp.kyoto-u.ac.jp

doi: 10.1096/fj.201801783RR
This article includes supplemental data. Please visit *http://www.fasebj.org* to obtain this information.

We show here that deletion of SKIP improves glucose tolerance through increasing not only insulin secretion but also GIP and GLP-1 secretions. In addition, depletion of SKIP improves lipid metabolism and reduces basal inflammation levels.

MATERIALS AND METHODS

Animals

Maintenance of the mice and all experimental procedures were conducted in accordance with the ethical guidelines of Kyoto University and approved by the Animal Research Committee, Graduate School of Medicine, Kyoto University. $SKIP^{-/-}$ mice, GIP-green fluorescent protein KI [GIP-GFP KI ($GIP^{gfp/gfp}$)] mice, and SKIP-mCherry KI/GIP-GFP KI ($SKIP^{-/-}GIP^{gfp/gfp}$) mice and wild-type (WT) littermates were used in all experiments. $SKIP^{-/-}$ mice, GIP-GFP KI hetero ($GIP^{gfp/+}$) mice, and glucagon-GFP KI hetero ($Gcg^{gfp/+}$) mice were generated as previously described (15–17). All animals were maintained under conditions of a 12-h light/dark cycle, with free access to water and food unless indicated otherwise. All mice used in individual experiments were age-matched at the beginning of the experiments. Bodyweight change and food intake were recorded weekly.

Isolation of K- and L-cells from mouse intestinal epithelium

Mouse upper, lower small intestine and colon samples were removed and washed with PBS. The procedure of isolation and collection of K- and L-cells from murine intestinal epithelium was previously described (17). GFP-positive and GFP-negative cells in the intestinal epithelium were analyzed using the BD FACS Aria II Flow Cytometer (BD Biosciences, San Jose, CA, USA). Sorted cells were collected in medium-containing vials at a rate of 2000 cells/tube for RT-PCR.

Oral glucose tolerance test and measurement of insulin, GIP, and GLP-1

Following 18 h without feeding, we administered 2 g/kg glucose or 6 g/kg glucose (for GLP-1 measurement) orally to WT, $SKIP^{-/-}$, $GIP^{gfp/gfp}$, and $SKIP^{-/-}GIP^{gfp/gfp}$ mice (age 12–16 wk) using a gavage tube. Blood glucose levels were measured by the glucose oxidase method (Sanwa Kagaku Kenkyusho, Nagoya, Japan). After collection, blood samples were kept on ice and then centrifuged (3000 rotations/minute for 10 min at 4°C), and plasma was separated. The plasma samples were used fresh or kept at −80°C until further processing. Insulin, total GIP, and GLP-1 levels were measured by ELISA as follows: Insulin Kit (Morinaga, Tokyo, Japan), total GIP Kit (MilliporeSigma, Burlington, MA, USA), and GLP-1 Kit (Meso Scale Discovery, Rockville, MD, USA).

Insulin tolerance test

Mice were unfed for 4 h before the start of the experiment; 0.5 U/kg of human insulin (100 U/ml; Eli Lily and Company, Indianapolis, IN, USA) was administered intraperitoneally. Blood samples were drawn from the tail at 0, 30, 60, and 120 min after insulin administration. Blood glucose levels were measured by the glucose oxidase method (Suzuken, Nagoya, Japan).

Biochemical analysis

Mice were unfed for 18 h and blood samples were collected from the tail veins. Levels of plasma triglyceride (Tg), total cholesterol (T-Cho), VLDL cholesterol (VLDL-Cho), LDL cholesterol (LDL-Cho), and HDL cholesterol (HDL-Cho) were measured using high-performance liquid chromatography (Skylight Biotech, Akita, Japan) as previously described (18). Nonesterified fatty acid (NEFA) levels were measured by enzymatic colorimetric assays (Wako Pure Chemicals, Osaka, Japan) after the mice were unfed overnight. Plasma adiponectin levels and leptin levels were determined using a mouse adiponectin sandwich enzyme immunoassay (BioVendor Research and Diagnostic Products, Brno, Czech Republic) and a Leptin ELISA Kit (Morinaga), respectively. Fasting plasma sphingosine kinase activity was assayed using a Sphingosine Kinase Activity Assay Kit (Echelon, San Jose, CA, USA). Plasma IL-6 and TNF-α levels were measured by Mouse IL-6 and TNF-α High Sensitivity ELISA Kits, respectively (Thermo Fisher Scientific, Waltham, MA, USA).

Measurement of body fat composition

The body fat was measured by a computed tomography (CT) scan (A La Theta LCT-100; Hitachi Aloka, Tokyo, Japan). The scanned area of the body was flanked by the xiphisternum and sacrum; the width of the scanned slices was 2 mm. The obtained images were analyzed by A La Theta software, v.1.00, and values for body fat, both subcutaneous and visceral fat, were quantified in grams.

Indirect calorimetry and mouse activity

Indirect calorimetry was performed, and the activity of the mice was measured (Arco 2000 mass spectrometer; Arco System, Chiba, Japan). Each mouse was placed in an individual chamber with free access to water. Energy expenditure (calories/min/kg), fat oxidation (mg/min/kg), and locomotor activity (counts/min) were measured every 5 min over 48 h.

Tissue collection

On the last day of the study, the mice were euthanized under whole-body inhalable anesthesia. The white adipose tissues (perirenal, mesenteric, epididymal) and other organs were harvested and measured; some parts were flash frozen in liquid nitrogen for RNA extraction and other parts were fixed in either paraformaldehyde or Bouin's solution for histologic analysis.

Quantitative analysis of mRNA expression

Total RNA was isolated using Trizol Reagent (Thermo Fisher Scientific). cDNA was synthesized using a PrimeScript RT Reagent Kit (Takara, Kyoto, Japan) according to the manufacturer's instructions. Quantitative RT-PCR (qRT-PCR) was performed using ribosomal protein S18 as an internal standard on the basis of the ABI Prism 7000 Sequence Detection System (AB StepOne Plus Real-Time PCR; Thermo Fisher Scientific). SYBR Green PCR Master Mix (Thermo Fisher Scientific) was prepared for PCR runs. Thermal cycling conditions were denatured at 95°C for 10 min, followed by 40 cycles at 95°C for 15 s and 60°C for 1 min. Primer pairs for PCR are listed in Supplemental Table S1.

Histologic analysis

All tissues except for intestines and pancrea were fixed in 4% paraformaldehyde in PBS overnight at 4°C and then embedded

in paraffin blocks. Intestines and pancrea were fixed in Bouin's solution and transferred into 70% ethanol before being processed through paraffin. Embedded tissues were sliced and deparaffinized with a series of xylene and ethanol. Mouse anti-mCherry antibody (ab125096, 1: 250; Abcam, Cambridge, MA, USA), rabbit anti-GIP antibody (T-4053, 1:100; Peninsula Laboratories, San Carlos, CA, USA), and rabbit anti-GLP-1 antibody (aa 1–19; HAEGTFTSDVSSYLEGQAAKC; generated by MilliporeSigma) were used for immunostaining. Liver and adipose tissue were embedded in paraffin and then stained with hematoxylin and eosin (H&E) staining. After immunostaining, for quantification of the adipocyte area, 15–20 adipocytes per section were averaged and images were analyzed by BZ Analyzer software (Keyence, Osaka, Japan).

Hepatic Tg content

Hepatic lipids were extracted as previously described (19). In brief, frozen liver tissues were homogenized and transferred into chloroform/methanol solution (2:1). The samples were then centrifuged for 10 min and the lipid-containing phase was removed. Finally, samples were dried under nitrogen gas and reconstituted with water. Tg levels were measured using commercial kits (Sekisui Medical, Tokyo, Japan). Hepatic lipid content was defined as per gram of the liver tissue weight.

Systolic blood pressure and heart rate measurement

Systolic blood pressure and heart rate were measured by a tail-cuff method (MK-2000ST; Muromachi Kikai, Tokyo, Japan). At least 6 readings were taken for each measurement.

Exendin-(9–39) administration

Alzet miniosmotic pumps (model 2004; Alzet, Cupertino, CA, USA) were implanted subcutaneously into both WT mice and $SKIP^{-/-}$ mice at 9 wk old. These mice were randomly divided into 4 groups and administered vehicle (0.9% NaCl, 1% bovine serum albumin) or exendin-(9–39) (150 pM/kg bodyweight/min; Abcam) for 4 wk.

Statistics

Comparison between 2 groups was performed using Student's *t* test or ANOVA with Bonferroni *post hoc* test. A 1-way ANOVA with Bonferroni's multiple comparisons test was performed when comparing more than 2 groups. A value of $P < 0.05$ was considered to be significant. Data are expressed as means ± SEM.

RESULTS

SKIP is expressed in enteroendocrine K- and L-cells

We found that SKIP was expressed not only in pancreatic β-cells but also in intestinal endocrine K-cells and L-cells. $GIP^{gfp/+}$ and $Gcg^{gfp/+}$ mice were generated for the purpose of visualizing enteroendocrine K-cells and L-cells, respectively (16, 17). Subsequently, GFP-positive cells and GFP-negative cells were separated and collected by flow cytometry. mRNA expression of proGIP and proglucagon were highly enriched in GFP-positive cells compared with those in negative cells from $GIP^{gfp/+}$ mice and $Gcg^{gfp/+}$ mice, indicating successful purification of K- and L-cells by flow cytometry (**Fig. 1*A***). Microarray analysis data revealed that SKIP mRNA levels were highly expressed in GFP-positive cells of both $GIP^{gfp/+}$ and $Gcg^{gfp/+}$ mice (15.82-fold and 3.48-fold, respectively) compared with those in GFP-negative cells (Supplemental Table S2). qRT-PCR also showed that expression levels of SKIP mRNA in the upper small intestine and colon were significantly higher by 8.5-fold and 2.1-fold, respectively, in GFP-positive cells compared with those in GFP-negative cells from both $GIP^{gfp/+}$ and $Gcg^{gfp/+}$ mice (Fig. 1*A*). We then ascertained whether SKIP was expressed in K- and L- cells by using $SKIP^{-/-}$ mice. SKIP expression was found to be decreased by about 80% in the upper and lower small intestine and colon in $SKIP^{-/-}$ mice (Fig. 1*B*). Immunohistochemical staining of $SKIP^{-/-}$ mice revealed that mCherry and GIP (Fig. 1*C*) or GLP-1 (Fig. 1*D*) were coexpressed almost entirely in the same cells of the intestine, indicating that SKIP is expressed in both K- and L-cells. This evidence suggests that SKIP could contribute to whole-body glucose homeostasis as well as to having other beneficial metabolic effects.

$SKIP^{-/-}$ mice show increased bodyweight

Starting from 6 wk of age, $SKIP^{-/-}$ mice fed standard chow showed a significant increase in bodyweight compared with that of WT mice (Fig. 1*E*). There was no difference in food intake between the 2 groups (Fig. 1*F*). The body temperature of $SKIP^{-/-}$ mice was significantly lower compared with that of WT mice (Fig. 1*G*). A CT scan revealed that subcutaneous, visceral, and total body fat mass in $SKIP^{-/-}$ mice were significantly increased compared with those in WT mice (Fig. 1*H*). The weight of epididymal, perirenal, and mesenteric adipose tissues in $SKIP^{-/-}$ mice were also markedly higher than those in WT mice (Fig. 1*I*). To investigate the mechanism underlying the increase in bodyweight, energy metabolism was evaluated. $SKIP^{-/-}$ mice showed a significant increase in fat oxidation (Fig. 1*J*) and a decrease in energy expenditure (Fig. 1*K*) compared with those in WT mice. Locomotor activity showed no significant changes (Fig. 1*L*). Western blot analysis revealed that SKIP was not detected in adipose tissues (Supplemental Fig. S1).

Insulin and incretin secretion are augmented in $SKIP^{-/-}$ mice

We next investigated whether or not loss of SKIP in mice affected glucose tolerance. During the oral glucose tolerance test (OGTT), blood glucose levels in $SKIP^{-/-}$ mice were lower than those in WT mice at both 15 and 30 min (**Fig. 2*A***). Area under the curve (AUC)-glucose was decreased by about 20% in $SKIP^{-/-}$ mice compared with that in WT mice. In addition, plasma insulin levels (Fig. 2*B*) in $SKIP^{-/-}$ mice were significantly higher in comparison with that in WT mice at 15 min. Compared with WT mice, $SKIP^{-/-}$ mice also showed an increase in total GIP levels at

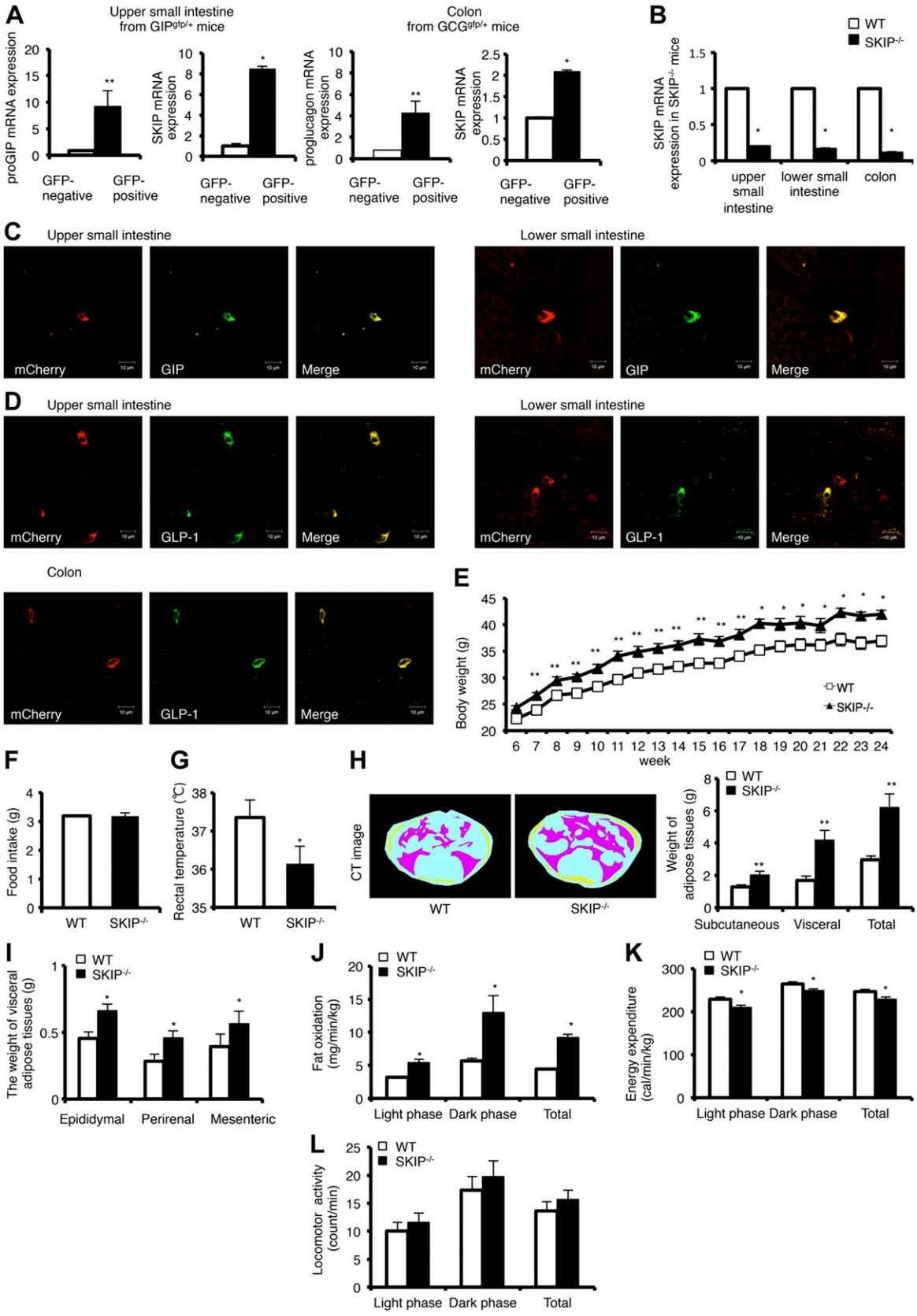

Figure 1. SKIP expression in intestinal K-cells and L-cells and SKIP$^{-/-}$ mice display adiposity. WT mice are represented by white bars and squares. SKIP$^{-/-}$ mice are represented by black bars and triangles. *A*) Real-time quantitative PCR analysis of proGIP mRNA and SKIP mRNA in GFP-negative cells (white bars) and GFP-positive cells (black bars) from the small intestine of GIP$^{gfp/+}$ mice; proglucagon and SKIP mRNA expression in GFP-negative cells (white bars) and GFP-positive cells (black bars) from colon of Gcg$^{gfp/+}$ mice (n = 8). *B*) Relative expression of SKIP mRNA in intestine of SKIP$^{-/-}$ mice by qRT-PCR (n = 8). *C*, *D*)

(*continued on next page*)

both 15 and 30 min (Fig. 2*C*) as well as total GLP-1 levels at 15 min (Fig. 2*D*). In addition, AUC-insulin (Fig. 2*B*), AUC-GIP (Fig. 2*C*), and AUC-GLP-1 (for 30 min) (Fig. 2*D*) in SKIP$^{-/-}$ mice were increased about 1.3-fold, 1.5-fold, and 1.3-fold, respectively, compared with those in WT mice. Changes of glucose, insulin, GIP, and GLP-1 from basal were also consistent (Supplemental Fig. S2). Similar trends were observed in female mice (Supplemental Fig. S3). The blood glucose levels in response to 0.5 U/kg human insulin were similar between WT and SKIP$^{-/-}$ mice (Fig. 2*E*). Taken together, these results indicate that depletion of SKIP improves glucose tolerance by increasing both insulin and incretin secretion without a change in insulin resistance compared with WT mice.

Changes in metabolic parameters in SKIP$^{-/-}$ mice

Fasting (**Fig. 3*A***) and *ad libitum* blood glucose levels (Fig. 3*B*) and fasting plasma insulin levels (Fig. 3*C*) were not different between WT and SKIP$^{-/-}$ mice. SKIP$^{-/-}$ mice exhibited markedly decreased fasting plasma Tg, VLDL-Cho, and LDL-Cho levels, compared with those of WT mice, while not showing any significant changes in HDL-Cho or NEFA levels (**Table 1**). We also evaluated gene expression levels involved in liver lipid synthesis of WT and SKIP$^{-/-}$ mice. The mRNA levels of sterol regulatory element-binding protein -1c, acetyl-CoA synthetase, acetyl-CoA carboxylase, fatty acid synthase, and stearoyl-CoA desaturaseadenosine 1 did not differ between WT and SKIP$^{-/-}$ mice (Supplemental Fig. S4*A*). The mRNA levels of hydroxymethylglutaryl-CoA synthase were significantly decreased in SKIP$^{-/-}$ mice compared with those in WT mice (Supplemental Fig. S4*B*). Plasma leptin (Fig. 3*D*) and adiponectin (Fig. 3*E*) levels were significantly increased in SKIP$^{-/-}$ mice compared with those in WT mice. Liver weight (Fig. 3*F*) and hepatic Tg content (Fig. 3*G*) were not different between WT and SKIP$^{-/-}$ mice. Liver histology also was not different between the 2 mice not showing fatty liver (Fig. 3*H*). Heart rate (Fig. 3*I*) and blood pressure (Fig. 3*J*) showed no significant changes between WT and SKIP$^{-/-}$ mice.

Basal inflammatory levels are decreased in SKIP$^{-/-}$ mice

Obesity is characterized as a state of chronic low-grade systemic inflammation (20, 21). The expansion of adipose tissue produces adipocytokines or adipokines, which could trigger chronic low-grade inflammation and induce obesity-related diseases, such as fatty liver and impaired glucose tolerance. Many studies have also shown positive association between obesity indices and inflammatory markers (20, 22). Because SKIP$^{-/-}$ mice exhibited overweight, we focused on an involvement of SKIP in inflammation. In the liver of SKIP$^{-/-}$ mice, the proinflammatory cytokines IL-1β and IL-6 mRNA levels were significantly decreased compared with those in WT mice (Fig. 3*K*). On the other hand, the TNF-α mRNA level did not differ between these 2 mice. Adipose tissues of SKIP$^{-/-}$ mice showed that IL-1β and IL-6 mRNA levels were significantly lower than those of WT mice (Fig. 3*L*). Concurrently, the anti-inflammatory cytokine IL-10 and adiponectin mRNA levels were markedly increased in SKIP$^{-/-}$ mice compared with those in WT mice (Fig. 3*L*). The mRNA levels of macrophage infiltration markers, such as monocyte chemotactic protein-1, remained similar between the 2 groups (Fig. 3*M*). Furthermore, SKIP$^{-/-}$ mice also exhibited a significant decrease in IL-1β and IL-6 mRNA levels and an increase in IL-10 mRNA levels in both duodenum (Fig. 3*N*) and colon (Fig. 3*O*) compared with WT mice. Depletion of Sphk1 has been reported to decrease proinflammatory molecules and increase anti-inflammatory molecules (23). However, in our SKIP$^{-/-}$ mice model, there was no difference in either Sphk1 mRNA expression levels in liver and adipose tissue (Supplemental Fig. S5*A*) or Sphk activity in serum (Supplemental Fig. S5*B*) compared with those in WT mice.

GIP is essential for fat accumulation and weight gain in SKIP$^{-/-}$ mice

Considering the bodyweight change in SKIP$^{-/-}$ mice, we hypothesized that GIP may have a contributing effect on the phenotype of SKIP$^{-/-}$ mice. The differences observed in bodyweight between WT and SKIP$^{-/-}$ mice were reproducible (**Fig. 4*A***). SKIP$^{-/-}$GIP$^{gfp/gfp}$ mice gained less bodyweight than SKIP$^{-/-}$ mice, which remained comparable to WT mice and GIP$^{gfp/gfp}$ mice (Fig. 4*A*). Food intake was recorded in both light and dark phases and did not change among the 4 groups (Fig. 4*B*). The weight of different parts of adipose tissues (Fig. 4*C*) and the adipocyte size (Fig. 4*D*) remained consistent with the bodyweight change. SKIP$^{-/-}$ mice showed an increase in both the weight of adipose tissues and adipocyte size, but there was no difference among the other 3 groups. Fat oxidation (Fig. 4*E*) and energy expenditure (Fig. 4*F*) in SKIP$^{-/-}$GIP$^{gfp/gfp}$ mice were reversed to almost the same levels as those in WT mice, whereas there was no significant difference between GIP$^{gfp/gfp}$ and SKIP$^{-/-}$GIP$^{gfp/gfp}$ mice. Locomotor activity did not differ among these 4 groups (Fig. 4*G*).

Immunohistochemical images of intestine sections from SKIP$^{-/-}$ mice and WT mice (red: anti-mCherry; green: anti-GIP) (*C*) and anti-GLP-1 ($n = 5$) (*D*). Scale bars, 10 μm. *E–H*) Bodyweight changes (*E*), food intake (*F*), and rectal temperature (*G*) of WT and SKIP$^{-/-}$ mice were monitored. *H*) CT images of transverse abdominal sections were taken and visceral, subcutaneous, and total fat (g) (left) and the analysis of CT results (right) in WT and SKIP$^{-/-}$ mice were measured ($n = 8$). *I*) The weight of epididymal, perirenal, and mesenteric adipose tissues were evaluated after dissection. *J–L*) Fat oxidation (mg/min/kg) (*J*), energy expenditure (calories/min/kg) (*K*), and locomotor activity (counts/min) (*L*) were measured ($n = 6$). Values are means ± SEM. $^*P < 0.05$, $^{**}P < 0.01$ *vs.* GFP-negative cells [Student's *t* test (*A*, *B*); 2-way ANOVA with Bonferroni *post hoc* test (*E*)]; $^*P < 0.05$, $^{**}P < 0.01$ *vs.* WT mice [Student's *t* test (*F–L*)].

GIP does not contribute to amelioration of glucose tolerance and lipid profiles in SKIP$^{-/-}$ mice

Although GIP$^{gfp/gfp}$ mice showed a significant increase in blood glucose levels compared with WT mice during OGTT, depletion of SKIP reduced blood glucose levels at 30 min as well as AUC-glucose in SKIP$^{-/-}$GIP$^{gfp/gfp}$ mice (**Fig. 5*A***). Plasma insulin levels were markedly decreased in GIP$^{gfp/gfp}$ compared with WT mice, whereas depletion of SKIP enhanced plasma insulin levels and AUC-insulin in SKIP$^{-/-}$GIP$^{gfp/gfp}$ mice (Fig. 5*B*). GIP secretion was significantly increased in SKIP$^{-/-}$ mice but was eliminated in GIP$^{gfp/gfp}$ mice and SKIP$^{-/-}$GIP$^{gfp/gfp}$ mice (Fig. 5C). The enhancement of GLP-1 secretion by the depletion of SKIP was maintained in SKIP$^{-/-}$GIP$^{gfp/gfp}$ mice (Fig. 5*D*). Changes of glucose, insulin, GIP, and GLP-1 from basal were also consistent (Supplemental Fig. S6). An insulin tolerance test (ITT) did not show any significant differences in insulin sensitivity among 4 groups (Fig. 5*E*). Elevated fasting plasma levels of leptin and adiponectin were reverted in SKIP$^{-/-}$GIP$^{gfp/gfp}$ mice to the levels of WT mice and GIP$^{gfp/gfp}$ mice (Fig. 5*F*, *G*). Reduced fasting plasma levels of Tg and LDL-Cho were still observed in SKIP$^{-/-}$GIP$^{gfp/gfp}$ mice compared with those in WT mice and GIP$^{gfp/gfp}$ mice (Fig. 5*H*, *I*).

GIP contributes to suppression of basal inflammation in SKIP$^{-/-}$ mice

Recently, the role of GIP/GIP receptor signaling in inflammation has been reported (24, 25). However, no

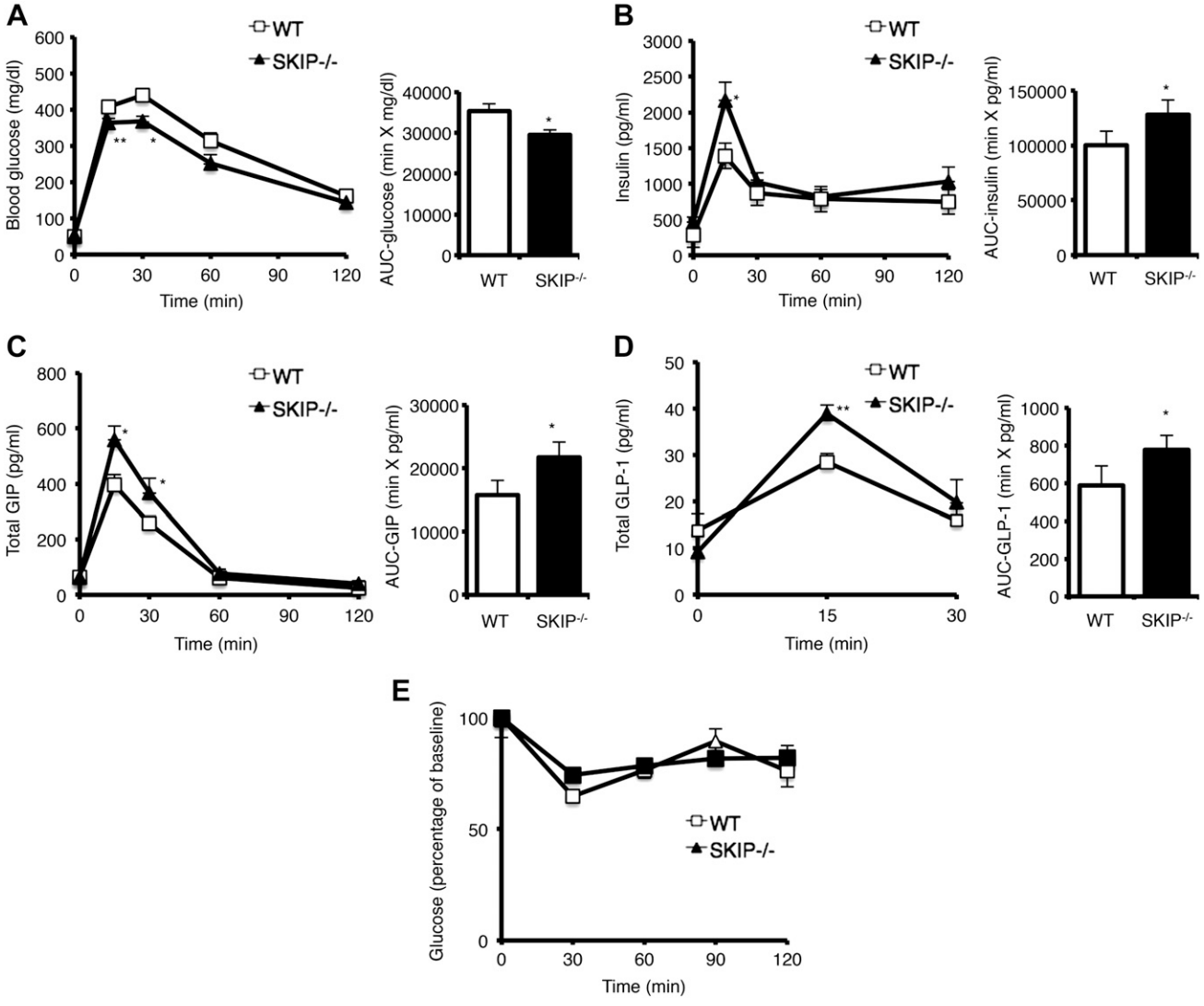

Figure 2. SKIP$^{-/-}$ mice show improved glucose tolerance by increasing insulin and incretin secretion. WT mice are represented by white bars and squares. SKIP$^{-/-}$ mice are represented by black bars and triangles. *A–D*) Blood glucose (*A*), insulin (*B*), total GIP (*C*), and GLP-1 levels (6 g/kg glucose) (*D*) during 2 g/kg glucose OGTT in WT and SKIP$^{-/-}$ mice. *E*) ITT was performed after injection of 0.5 U/kg insulin into WT and SKIP$^{-/-}$ mice. The levels of blood glucose at a series of time points were measured and normalized to the basal point (0) ($n = 8$). Values are means ± SEM. $^*P < 0.05$, $^{**}P < 0.01$ *vs.* WT mice (2-way ANOVA with Bonferroni *post hoc* test or Student's *t* test).

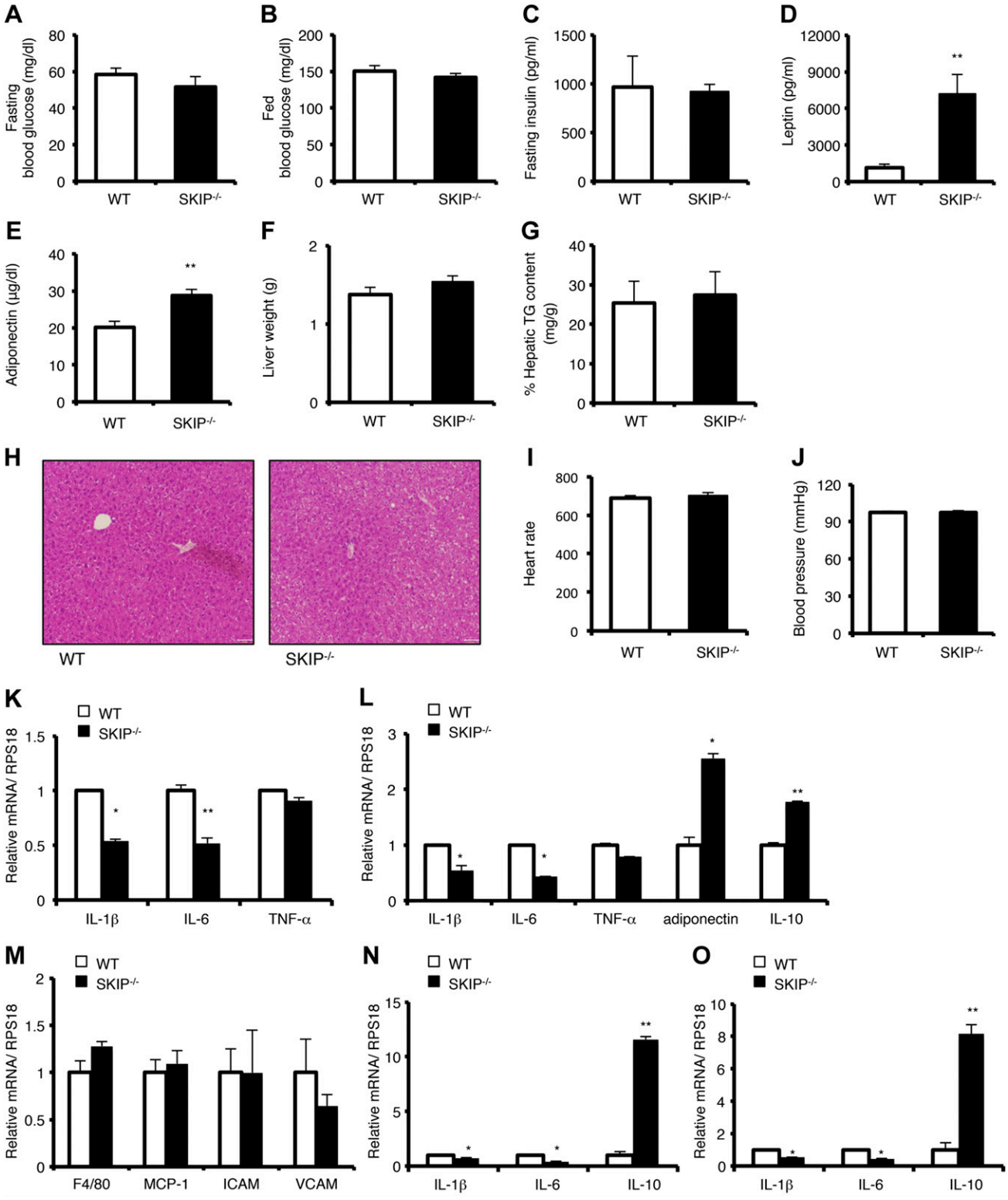

Figure 3. SKIP$^{-/-}$ mice exhibit increased leptin and adiponectin levels and decreased basal inflammation levels without other metabolic changes. WT mice are represented by white bars. SKIP$^{-/-}$ mice are represented by black bars. *A–E*) Unfed (*A*), fed blood glucose (*B*), fasting insulin (*C*), plasma leptin (*D*), and plasma adiponectin levels (*E*) of WT and SKIP$^{-/-}$ mice ($n = 8$). *F–H*) Liver weight (*F*), liver Tg content (*G*), and H&E staining (*H*) of WT and SKIP$^{-/-}$ mice. Scale bar, 64 μm (*H*). *I, J*) Heart rate (*I*) and blood pressure (*J*) of WT and SKIP$^{-/-}$ mice; $n = 6$. *K*) The expression of proinflammatory markers in liver by qRT-PCR. *L, M*) The expression of proinflammatory markers (*L*) and adipokines and macrophage markers (*M*) in adipose tissues. *N, O*) The expression of IL-1β, IL-6, and IL-10 in duodenum (*N*) and colon (*O*) between WT and SKIP$^{-/-}$ ($n = 4$). Values are means ± SEM. $^*P < 0.05$, $^{**}P < 0.01$ *vs.* WT mice (Student's *t* test).

TABLE 1. *Fasting plasma lipid levels in WT and SKIP$^{-/-}$ mice*

Variable	WT	SKIP$^{-/-}$	*P*
Tg (mg/dl)	178.0 ± 15.0	123.8 ± 4.7	0.030
VLDL-Cho (mg/dl)	13.0 ± 1.5	9.1 ± 1.5	0.010
LDL-Cho (mg/dl)	13.7 ± 1.5	11.4 ± 1.4	0.032
HDL-Cho (mg/dl)	74.8 ± 15.3	88.0 ± 6.9	0.203
NEFA (μEq/L)	635.0 ± 52.3	676.2 ± 33.4	0.152

All data are expressed as means ± SE ($n = 6$). Data were analyzed by Student's *t* test. A significant difference was considered at $P < 0.05$.

studies have shown a direct relationship between GIP and basal inflammation under regular chow diet rather than a high fat diet. Here, we investigated the role of GIP in basal inflammation of SKIP$^{-/-}$ mice under regular chow diet. Interestingly, the suppression of the proinflammatory cytokine IL-6 by the depletion of SKIP in liver was reverted in SKIP$^{-/-}$GIP$^{gfp/gfp}$ mice to the levels of WT mice and GIP$^{gfp/gfp}$ mice (**Fig. 6*A***). Suppression of IL-1β and IL-6 and elevation of adiponectin and anti-inflammatory cytokine IL-10 by depletion of SKIP in adipose tissues were reverted in SKIP$^{-/-}$GIP$^{gfp/gfp}$ mice to the levels of WT mice and GIP$^{gfp/gfp}$ mice (Fig. 6*B*). mRNA expression of macrophage infiltration markers in adipose tissue remained unchanged (Fig. 6*C*). Suppression of IL-1β and IL-6 and elevation of IL-10 by depletion of SKIP in duodenum and colon were reverted in SKIP$^{-/-}$GIP$^{gfp/gfp}$ mice to the levels of WT mice and GIP$^{gfp/gfp}$ mice (Fig. 6*D, E*). Consistent with the change in expression of IL-6 mRNA, the reductions of plasma IL-6 levels by depletions of SKIP were reverted to the levels of WT mice and GIP$^{gfp/gfp}$ mice (Fig. 6*F*). Plasma TNF-α levels did not change among the 4 groups (Fig. 6*G*).

GLP-1 contributes to amelioration of glucose tolerance and lipid profiles in SKIP$^{-/-}$ mice

To clarify the role of GLP-1 on SKIP$^{-/-}$ mice, exendin-(9–39), an antagonist of the GLP-1 receptor, was administered from 9 wk of age *via* an Azlet miniosmotic subcutaneous pump for 4 wk. Exendin-(9–39) treatment had no effect on either bodyweight or food intake in WT mice and SKIP$^{-/-}$ mice (**Fig. 7*A, B***). However, *ad libitum* blood glucose levels were significantly higher in exendin-(9–39)-treated WT mice and SKIP$^{-/-}$ mice at both the first and last weeks of treatment compared with those in vehicle-treated WT mice and SKIP$^{-/-}$ mice (Fig. 7*C*). After an oral load of 6 g/kg glucose, exendin-(9–39) administration did not affect glucose tolerance in WT mice but completely abolished the effects of SKIP depletion on glucose tolerance during 30 min (Fig. 7*D*). Exendin-(9–39) administration enhanced GLP-1 secretion in WT mice, but more so in SKIP$^{-/-}$ mice (Fig. 7*E*). This effect was underlain by the ability of exendin-(9–39) to antagonize the incretin effect of GLP-1. Changes of glucose and GLP-1 from basal were also consistent (Supplemental Fig. S7). Because the GLP-1 action was blocked by exendin-(9–39), we examined gene expression levels involved in inflammation because GLP-1 also has an anti-inflammatory effect (26). The suppression of IL-1β, IL-6, and TNF-α by depletion of SKIP in the liver was not affected by exendin-(9–39) administration (Fig. 7*F*). On the other hand, suppression of IL-1β and elevation of adiponectin and IL-10 by depletion of SKIP in adipose tissue were cancelled by exendin-(9–39) administration (Fig. 7*G*). The fasting plasma levels of Tg and LDL-Cho were not affected by exendin-(9–39) administration in WT mice (Fig. 7*H, I*). However, in SKIP$^{-/-}$ mice, exendin-(9–39) administration reverted the levels of Tg and LDL-Cho to the levels of WT mice.

DISCUSSION

SKIP was recently identified as a novel regulator of glucose-stimulated insulin secretion (15). We have previously found that SKIP is highly expressed in pancreatic β-cells and that depletion of SKIP amplifies glucose-stimulated insulin secretion. Interestingly, SKIP is also highly expressed in intestinal K-cells and L-cells. We here provide the first evidence that SKIP regulates not only insulin secretion but also GIP and GLP-1 secretion. Although global depletion of SKIP slightly increased bodyweight and adipose tissue mass, glucose tolerance was better in SKIP$^{-/-}$ mice than that in WT mice without changes in both insulin sensitivity and fatty liver. In addition, plasma Tg, VLDL-Cho, and LDL-Cho levels were reduced, plasma adiponectin levels were elevated, and basal inflammation in the liver, adipose tissues, and the intestine were decreased in SKIP$^{-/-}$ mice compared with those in WT mice.

Obesity is known to be accompanied by low-grade systemic inflammation. Moreover, GIP is an important mediator of fat accumulation and obesity (27); the blood GIP level is elevated in obesity (28). Although SKIP$^{-/-}$ mice displayed overweight and increased GIP levels during OGTT, basal inflammation levels in the liver, adipose tissues, and intestine were lower than those in WT mice. We also evaluated the effect of SKIP deletion on bodyweight regulation in the absence of GIP secretion to investigate the direct action of GIP. After diminishing both SKIP and GIP action by making SKIP$^{-/-}$GIP$^{gfp/gfp}$ mice, the bodyweight, fat mass, plasma insulin levels, plasma adiponectin, and local inflammation levels in SKIP$^{-/-}$GIP$^{gfp/gfp}$ mice were found to be reversed and were comparable with those in WT mice. However, bodyweight, fat accumulation, and basal inflammation were comparable between GIP$^{gfp/gfp}$ and SKIP$^{-/-}$GIP$^{gfp/gfp}$ mice despite GIP depletion. These findings demonstrate that SKIP depletion contributes to both adiposity and inflammation in a GIP-dependent manner. Previous studies have shown that increased GIP signaling under either administration of pharmacological GIP concentration or stimulation of GIP secretion by high fat diet loading plays an important role in inflammation. However, to our knowledge, this is the first report to show that elevated GIP levels within the physiologic range significantly inhibit basal proinflammatory gene expression.

Although overweight is often associated with impaired glucose tolerance, SKIP$^{-/-}$ mice showed improvement of glucose tolerance because of the enhanced insulin

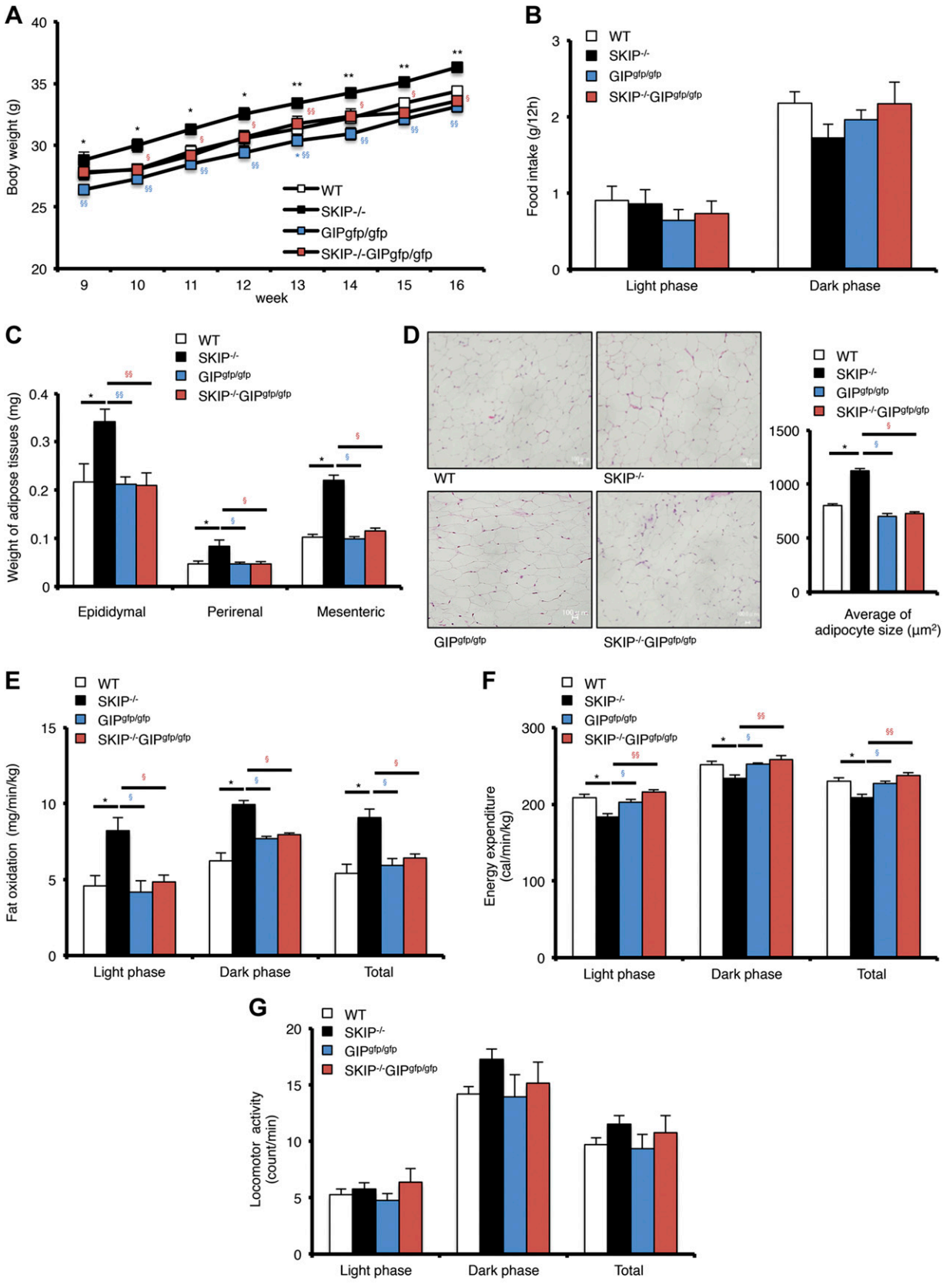

Figure 4. GIP is essential for adiposity in SKIP$^{-/-}$ mice. WT mice are represented by white bars and squares; SKIP$^{-/-}$ mice are represented by black bars and squares; GIP$^{gfp/gfp}$ mice are represented by blue bars and squares; SKIP$^{-/-}$GIP$^{gfp/gfp}$ mice are represented by red bars and squares. *A*, *B*) Bodyweight changes (*A*) and diurnal rhythm of food intake (*B*) among WT, SKIP$^{-/-}$, GIP$^{gfp/gfp}$, and SKIP$^{-/-}$GIP$^{gfp/gfp}$ mice (n = 8). *C*) The weight of epididymal, perirenal, and mesenteric adipose tissues were

(*continued on next page*)

secretion and the suppression of basal inflammation. It is suggested that improvement of glucose tolerance in SKIP$^{-/-}$ mice is mainly mediated by enhanced secretion of GLP-1, not GIP, as demonstrated using genetic deletion of GIP or pharmacological inhibition of GLP-1 signaling (Figs. 5 and 7). Because GLP-1 and GIP are both responsible for enhancement of insulin secretion (29), it is of interest to investigate why GLP-1 primarily plays a role in amelioration of glucose tolerance by depletion of SKIP.

Dyslipidemia is a major risk factor for cardiovascular diseases that are still the leading cause of death around the world (30). Lipid abnormalities include hypertriacylglycerolaemia, increased levels of small dense LDL, and low levels of HDL (8). In our SKIP$^{-/-}$ mice model, plasma Tg, VLDL-Cho, and LDL-Cho levels were significantly lower than those in WT mice. However, even with eliminated GIP expression in SKIP$^{-/-}$ mice, Tg and LDL-Cho levels still remained at the lower levels of SKIP$^{-/-}$ mice compared with WT mice. GIP$^{gfp/gfp}$ mice showed increased levels compared with SKIP$^{-/-}$GIP$^{gfp/gfp}$ mice, indicating that GIP might not be involved in a role of regulating lipid metabolism in SKIP$^{-/-}$ mice.

Recently, GLP-1 has received attention not only as an antidiabetic therapy for regulating hyperglycemia but also as a regulator of lipid and lipoprotein metabolism (31). It has been reported that GLP-1 agonists and dipeptidyl peptidase-4 inhibitors decreased Tg and T-Cho levels (8, 10, 11). Moreover, accumulating evidence shows that GLP-1 exhibits effects on anti-inflammation in adipose tissues and nonalcoholic fatty liver, thereby contributing to lower glucose levels in diabetes (26, 32–35). Thus, increased secretion of GLP-1 also may contribute to improved glucose homeostasis, lipid profiles, and alleviation of basal inflammation observed under depletion of SKIP. Exendin-(9–39), a derivative of the nonmammalian peptide of exendin-4, has been found to act as a specific and competitive antagonist on the GLP-1 receptor and impairs glucose tolerance in both humans and some animal models (36). Here, we administered exendin-(9–39) as a continuous infusion to inhibit GLP-1 action to investigate the effect of GLP-1 on SKIP$^{-/-}$ mice. Treatment with exendin-(9–39) significantly increased both fasting and fed blood glucose levels in SKIP$^{-/-}$ mice without alteration of bodyweight and food intake. The mRNA level of IL-1β in adipose tissue was significantly increased in exendin-(9–39)-treated mice compared with that in vehicle-treated mice. Plasma Tg and LDL-Cho levels also were markedly increased in exendin-(9–39)-treated mice compared with those in vehicle-treated mice. These observations suggest a beneficial role of GLP-1 in terms of both alleviation of inflammation and lipid metabolism in SKIP$^{-/-}$ mice. The current study failed to elucidate molecular mechanisms of GLP-1 regulation of inflammation and lipid metabolism; how GLP-1 exerts biologic effects in peripheral tissues lacking GLP-1 receptor expression remains unknown (36) and requires further investigation.

Adiponectin is an adipokine that acts as a protective insulin-sensitizing factor that can alleviate obesity-induced insulin resistance (37). Adiponectin levels are negatively associated with mediators of inflammation including IL-6 and C-reactive protein, but are positively related to anti-inflammatory cytokine IL-10 (38, 39). Compelling evidence also suggests that adiponectin-overexpressing transgenic ob/ob mice exhibit obesity but with improved glucose tolerance and reduced circulating Tg levels (40). In addition, hyperadiponectinaemia is associated with improved metabolic profiles of obese subjects (41–44). Increased adiponectin levels also are associated with better glycemic control, better lipid profile, and reduced inflammation in diabetic subjects (45, 46). Interestingly, unlike in other animal obesity models, both the plasma and mRNA levels in adipose tissues of adiponectin in SKIP$^{-/-}$ mice were significantly increased. Thus, increased adiponectin levels may partially contribute to better metabolic conditions and lowered basal inflammation levels in SKIP$^{-/-}$ mice.

SKIP$^{-/-}$ mice showed a significant decrease in body temperature and reduced energy expenditure, which may indicate the impairment of thermogenesis. It was previously shown that IL-6 is involved in body temperature regulation during both infection and long-term cold exposure (37). Our SKIP$^{-/-}$ mice had lower IL-6 levels compared with WT mice, which might also partly explain the lower body temperature. However, how SKIP deficiency results in the decrease in body temperature and its physiologic relevance awaits further investigations.

Previous studies have also demonstrated that SKIP interacts with Sphk1 and inhibits sphingosine kinase activity (14). Sphk1 phosphorylates sphingosine to form sphingosine 1 phosphate, a bioactive sphingolipid with numerous roles in inflammation (47, 48). In diet-induced obese mice, Sphk1 deficiency increased markers of adipogenesis and adipose gene expression of the anti-inflammatory molecules and reduced proinflammatory molecules in adipose tissue (23). In addition, loss of Sphk1 also predisposes to the onset of diabetes (49). However, we found that both plasma Sphk activity and Sphk1 mRNA levels in liver and adipose tissues were not different between SKIP$^{-/-}$ mice and WT mice. Our previous study also showed that Sphk activity in the islets was not different between WT and SKIP$^{-/-}$ mice (15).

It is important for the treatment of type 2 diabetes to improve glycemic control by promoting insulin secretion and ameliorating insulin resistance. Furthermore, management of the lipid profile and blood pressure is also essential to prevent diabetic complications. Therefore, a treatment that simultaneously promotes insulin secretion and incretin secretion accompanied with regulation of

evaluated after dissection. *D*) H&E staining of epididymal adipose tissue and adipocyte size of WT, SKIP$^{-/-}$, GIP$^{gfp/gfp}$, and SKIP$^{-/-}$GIP$^{gfp/gfp}$ mice ($n = 6$) Scale bars, 100 μm. *E–G*) Fat oxidation (mg/min/kg) (*E*), energy expenditure (calories/min/kg) (*F*), and locomotor activity (counts/min) (*G*) were measured ($n = 8$). Values are means ± SEM. $^{*}P < 0.05$, $^{**}P < 0.01$ *vs.* WT mice; $^{§}P < 0.05$, $^{§§}P < 0.01$ *vs.* SKIP$^{-/-}$ mice.

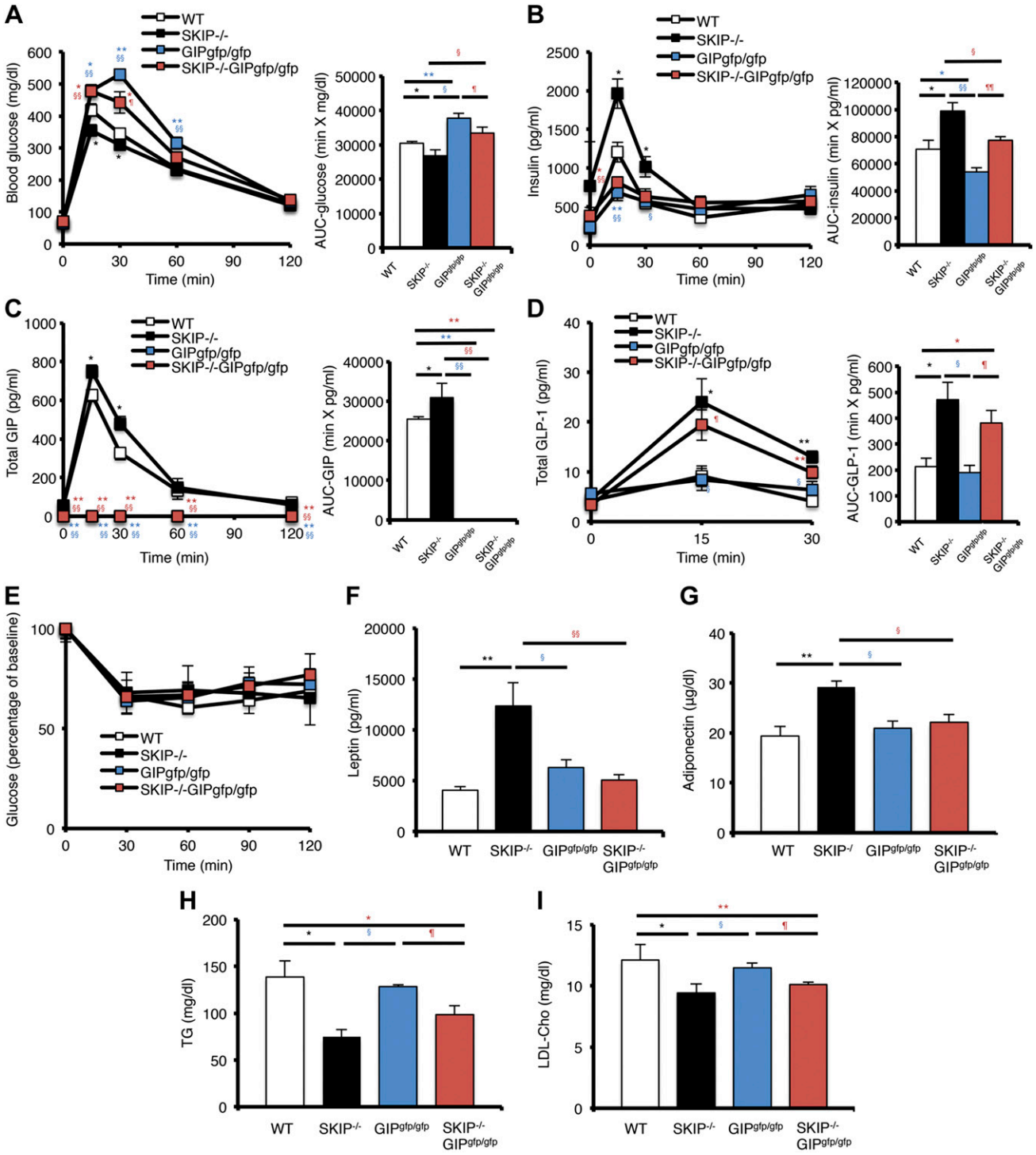

Figure 5. GIP does not contribute to improvement of glucose tolerance and lipids profile in SKIP$^{-/-}$ mice. WT mice are represented by white bars and squares, SKIP$^{-/-}$ mice are represented by black bars and squares, GIP$^{gfp/gfp}$ mice are represented by blue bars and squares, SKIP$^{-/-}$GIP$^{gfp/gfp}$ mice are represented by red bars and squares. *A–D*) Blood glucose (*A*), insulin (*B*), total GIP levels (*C*), and GLP-1 levels (6 g/kg glucose) (*D*) during 2 g/kg glucose OGTT among WT, SKIP$^{-/-}$, GIP$^{gfp/gfp}$, and SKIP$^{-/-}$GIP$^{gfp/gfp}$ mice. *E*) ITT was performed after injection of 0.5 U/kg insulin into WT, SKIP$^{-/-}$, GIP$^{gfp/gfp}$, and SKIP$^{-/-}$GIP$^{gfp/gfp}$ mice. The levels of blood glucose at a series of time points were measured and normalized to the basal point (0) (n = 8). *F, G*) Fasting leptin (*F*) and adiponectin (*G*) levels. *H, I*) Fasting Tg (*H*) and LDL-Cho (*I*) levels among WT, SKIP$^{-/-}$, GIP$^{gfp/gfp}$, and SKIP$^{-/-}$GIP$^{gfp/gfp}$ mice (n = 8). Values are means ± SEM. $^{*}P < 0.05$, $^{**}P < 0.01$ *vs.* WT mice; $^{\S}P < 0.05$, $^{\S\S}P < 0.01$ *vs.* SKIP$^{-/-}$ mice; $^{\P}P < 0.05$, $^{\P\P}P < 0.01$ *vs.* GIP^{gfp}/^{gfp} mice (ANOVA with Bonferroni's multiple comparisons test).

lipid metabolism may be an ideal treatment for glycemic control and prevention of diabetic complications. The current study and our previous study (15) failed to reveal how SKIP deficiency enhances secretions of insulin and incretin; it warrants further investigations not only to better understand how SKIP regulates secretion of these

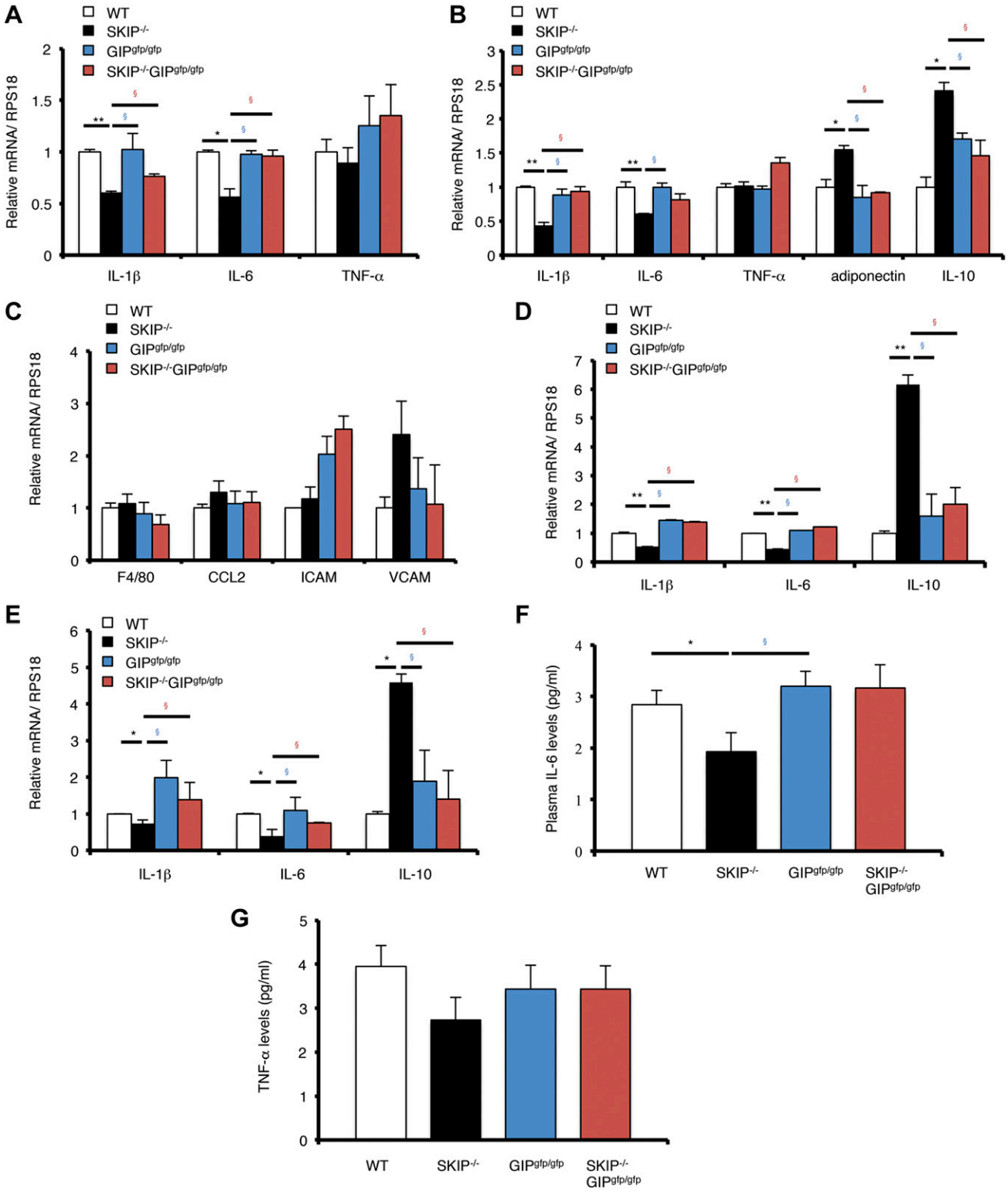

Figure 6. Basal inflammation levels in SKIP$^{-/-}$GIP$^{gfp/gfp}$ mice are reversed to the same levels of WT mice. WT mice are represented by white bars; SKIP$^{-/-}$ mice are represented by black bars; GIP$^{gfp/gfp}$ mice are represented by blue bars; SKIP$^{-/-}$GIP$^{gfp/gfp}$ mice are represented by red bars. *A*) The expression of proinflammatory markers in liver by qRT-PCR. *B*, *C*) The expression of inflammation (*B*) and macrophage (*C*) markers in adipose tissues. *D*, *E*) The expression of IL-1β, IL-6, and IL-10 in duodenum (*D*) and colon (*E*) among WT, SKIP$^{-/-}$, GIP$^{gfp/gfp}$, and SKIP$^{-/-}$GIP$^{gfp/gfp}$ mice ($n = 6$). RPS18, ribosomal protein S18. *F*, *G*) Plasma IL-6 (*F*) and plasma TNF-α (*G*) levels in WT, SKIP$^{-/-}$, GIP$^{gfp/gfp}$, and SKIP$^{-/-}$GIP$^{gfp/gfp}$ mice; $n = 8$. Values are means ± SEM. $^{*}P < 0.05$, $^{**}P < 0.01$ *vs.* WT mice; $^{\S}P < 0.05$, *vs.* SKIP$^{-/-}$ mice.

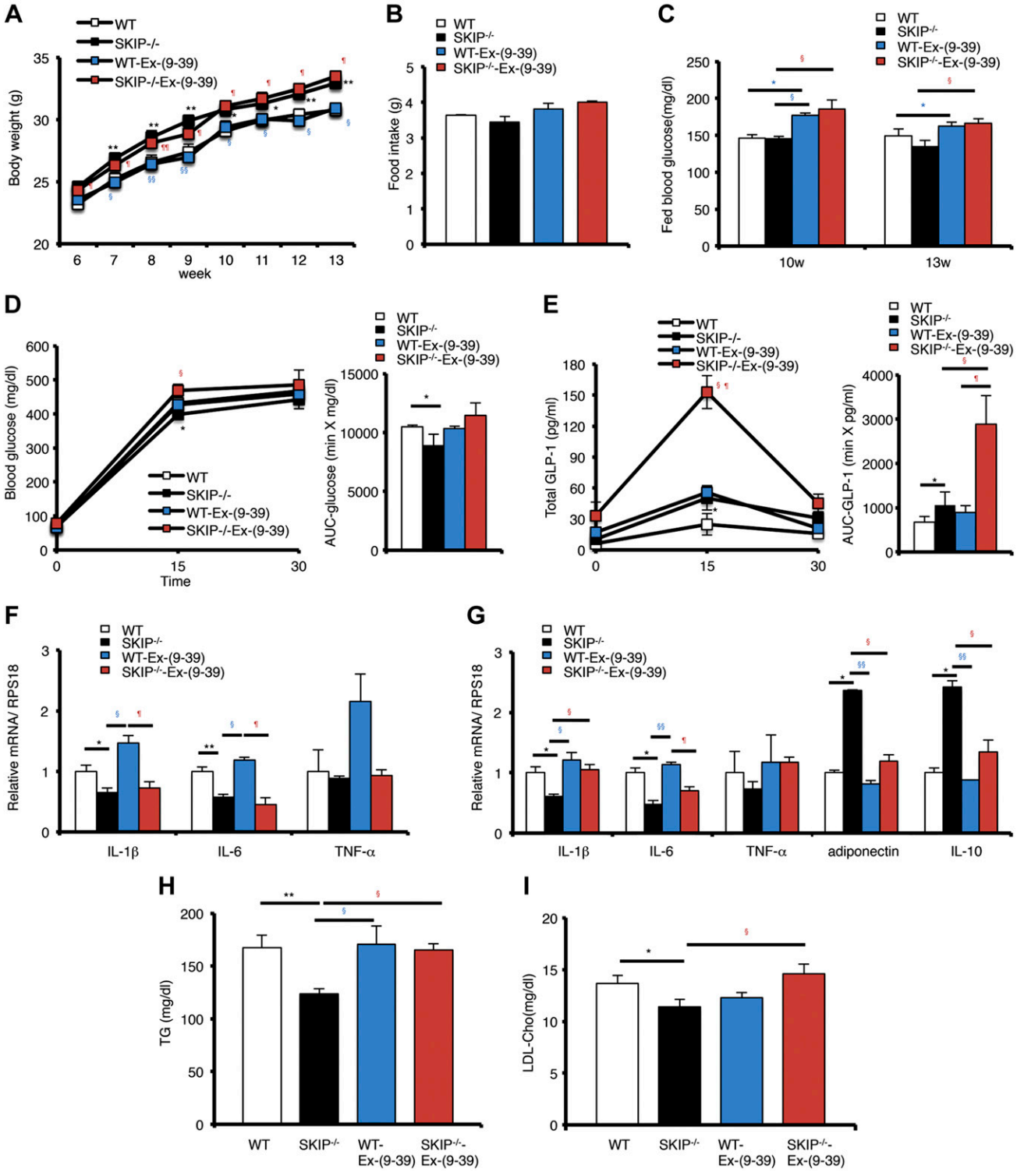

Figure 7. The blockade of GLP-1 action increases the expression of proinflammatory markers and plasma Tg levels. Vehicle-treated WT mice are represented by white bars and squares. Vehicle-treated SKIP$^{-/-}$ mice are represented by black bars and squares. Exendin-(9–39)-treated WT mice are represented by blue bars and blue squares. Exendin-(9–39)-treated SKIP$^{-/-}$ mice are represented by red bars and squares. *A–C*) Bodyweight (*A*), food intake (*B*), and blood glucose levels (*C*) in vehicle- and exendin-(9–39)-treated mice. *D, E*) Blood glucose (*D*) and total GLP-1 (*E*) levels of exendin-(9–39) and vehicle-treated WT and SKIP$^{-/-}$ mice in response to a 6 g/kg oral glucose load ($n = 6$). *F*) Liver gene expression involved in inflammation. *G*) The expression of proinflammatory and anti-inflammatory adipokines in adipose tissues of exendin-(9–39)- and vehicle-treated WT and SKIP$^{-/-}$ mice ($n = 5$). RPS18, ribosomal protein S18. *H, I*) Fasting Tg (*H*) and LDL-Cho (*I*) levels in exendin-(9–39)- and vehicle-treated WT and SKIP$^{-/-}$ mice ($n = 6$). Values are means ± SEM. $^{*}P < 0.05$, $^{**}P < 0.01$ *vs.* WT mice; $^{\S}P < 0.05$, $^{\S\S}P < 0.01$ *vs.* SKIP$^{-/-}$ mice; $^{\P}P < 0.05$, $^{\P\P}P < 0.01$ *vs.* WT-Ex- (9–39)-treated mice (ANOVA with Bonferroni's multiple comparisons test).

hormones but also to provide the molecular basis for potential therapeutics involving SKIP. In addition, the current study using whole-body SKIP knockout mice failed to exclude potential involvement of SKIP function in other tissues or cell types (15), which might be clarified by using tissue-specific SKIP$^{-/-}$ mice.

In summary, we have found that depletion of SKIP promotes both insulin and incretin secretion. SKIP$^{-/-}$ mice showed a slight increase in bodyweight, fasting plasma Tg, VLDL-Cho, and LDL-Cho levels, and basal inflammation levels in the liver, adipose tissues, and intestine were significantly decreased, resulting in more metabolically healthy conditions. Thus, inhibition of SKIP action may emerge as a new option for treatment of type 2 diabetes mellitus with metabolic dysfunction. FJ

ACKNOWLEDGMENTS

This work was supported by grants from the Japan Society for the Promotion of Sciences and Japan Agency for Medical Research and Development (AMED); Grants-in-Aid for Scientific Research (KAKENHI) Grants 24591325 (to S.H.), 18K08474 (to S.H.), 26111004 (to D.Y.), 17K09825 (to D.Y.), 17K19654 (to N.I.), and 16H05326 (to N.I.); and AMED Grants JP17lm0203006j0001 (to S.H.), 19ek0210111h0002 (to D.Y.), 17ek0210079h0001 (to N.I.). The authors declare no conflicts of interest.

AUTHOR CONTRIBUTIONS

Y. Liu and S. Harashima designed and performed all the experiments, contributed to discussion, and wrote, reviewed, and edited the manuscript; Y. Wang and K. Suzuki researched data and contributed to discussion; S. Tokumoto, R. Usui, and H. Tatsuoka performed the pump experiments and contributed to discussion; D. Tanaka contributed to discussion; D. Yabe and N. Harada contributed to discussion and analyzed data; Y. Hayashi provided materials and contributed to discussion; N. Inagaki contributed to discussion and wrote, reviewed, and edited the manuscript; N. Inagaki is the guarantor of this work and, as such, has full access to all the data in the study and takes responsibility for the integrity of the data and the accuracy of the data analysis; and all authors reviewed and approved the manuscript.

REFERENCES

1. Creutzfeldt, M. (1974) Candidate hormones of the gut. XV. Insulin-releasing factors of the gastrointestinal mucosa (Incretin). *Gastroenterology* **67**, 748–750
2. Schmidt, W. E., Siegel, E. G., and Creutzfeldt, W. (1985) Glucagon-like peptide-1 but not glucagon-like peptide-2 stimulates insulin release from isolated rat pancreatic islets. *Diabetologia* **28**, 704–707
3. Yamane, S., Harada, N., and Inagaki, N. (2016) Mechanisms of fat-induced gastric inhibitory polypeptide/glucose-dependent insulinotropic polypeptide secretion from K cells. *J. Diabetes Investig.* **7** (Suppl 1), 20–26
4. Eckel, R. H., Fujimoto, W. Y., and Brunzell, J. D. (1979) Gastric inhibitory polypeptide enhanced lipoprotein lipase activity in cultured preadipocytes. *Diabetes* **28**, 1141–1142
5. Tsukiyama, K., Yamada, Y., Yamada, C., Harada, N., Kawasaki, Y., Ogura, M., Bessho, K., Li, M., Amizuka, N., Sato, M., Udagawa, N., Takahashi, N., Tanaka, K., Oiso, Y., and Seino, Y. (2006) Gastric inhibitory polypeptide as an endogenous factor promoting new bone formation after food ingestion. *Mol. Endocrinol.* **20**, 1644–1651
6. Komatsu, R., Matsuyama, T., Namba, M., Watanabe, N., Itoh, H., Kono, N., and Tarui, S. (1989) Glucagonostatic and insulinotropic action of glucagonlike peptide I-(7-36)-amide. *Diabetes* **38**, 902–905
7. Willms, B., Werner, J., Holst, J. J., Orskov, C., Creutzfeldt, W., and Nauck, M. A. (1996) Gastric emptying, glucose responses, and insulin secretion after a liquid test meal: effects of exogenous glucagon-like peptide-1 (GLP-1)-(7-36) amide in type 2 (noninsulin-dependent) diabetic patients. *J. Clin. Endocrinol. Metab.* **81**, 327–332
8. Hsieh, J., Longuet, C., Baker, C. L., Qin, B., Federico, L. M., Drucker, D. J., and Adeli, K. (2010) The glucagon-like peptide 1 receptor is essential for postprandial lipoprotein synthesis and secretion in hamsters and mice. *Diabetologia* **53**, 552–561
9. Sun, F., Wu, S., Guo, S., Yu, K., Yang, Z., Li, L., Zhang, Y., Quan, X., Ji, L., and Zhan, S. (2015) Impact of GLP-1 receptor agonists on blood pressure, heart rate and hypertension among patients with type 2 diabetes: a systematic review and network meta-analysis. *Diabetes Res. Clin. Pract.* **110**, 26–37
10. Zhong, J., Maiseyeu, A., and Rajagopalan, S. (2015) Lipoprotein effects of incretin analogs and dipeptidyl peptidase 4 inhibitors. *Clin. Lipidol.* **10**, 103–112
11. Sun, F., Wu, S., Wang, J., Guo, S., Chai, S., Yang, Z., Li, L., Zhang, Y., Ji, L., and Zhan, S. (2015) Effect of glucagon-like peptide-1 receptor agonists on lipid profiles among type 2 diabetes: a systematic review and network meta-analysis. *Clin. Ther.* **37**, 225–241.e8
12. Kovanich, D., van der Heyden, M. A., Aye, T. T., van Veen, T. A., Heck, A. J., and Scholten, A. (2010) Sphingosine kinase interacting protein is an A-kinase anchoring protein specific for type I cAMP-dependent protein kinase. *ChemBioChem* **11**, 963–971
13. Scholten, A., Poh, M. K., van Veen, T. A., van Breukelen, B., Vos, M. A., and Heck, A. J. (2006) Analysis of the cGMP/cAMP interactome using a chemical proteomics approach in mammalian heart tissue validates sphingosine kinase type 1-interacting protein as a genuine and highly abundant AKAP. *J. Proteome Res.* **5**, 1435–1447
14. Lacaná, E., Maceyka, M., Milstien, S., and Spiegel, S. (2002) Cloning and characterization of a protein kinase A anchoring protein (AKAP)-related protein that interacts with and regulates sphingosine kinase 1 activity. *J. Biol. Chem.* **277**, 32947–32953
15. Wang, Y., Harashima, S. I., Liu, Y., Usui, R., and Inagaki, N. (2017) Sphingosine kinase 1-interacting protein is a novel regulator of glucose-stimulated insulin secretion. *Sci. Rep.* **7**, 779
16. Hayashi, Y., Yamamoto, M., Mizoguchi, H., Watanabe, C., Ito, R., Yamamoto, S., Sun, X. Y., and Murata, Y. (2009) Mice deficient for glucagon gene-derived peptides display normoglycemia and hyperplasia of islet alpha-cells but not of intestinal L-cells. *Mol. Endocrinol.* **23**, 1990–1999
17. Suzuki, K., Harada, N., Yamane, S., Nakamura, Y., Sasaki, K., Nasteska, D., Joo, E., Shibue, K., Harada, T., Hamasaki, A., Toyoda, K., Nagashima, K., and Inagaki, N. (2013) Transcriptional regulatory factor X6 (Rfx6) increases gastric inhibitory polypeptide (GIP) expression in enteroendocrine K-cells and is involved in GIP hypersecretion in high fat diet-induced obesity. *J. Biol. Chem.* **288**, 1929–1938
18. Usui, S., Hara, Y., Hosaki, S., and Okazaki, M. (2002) A new on-line dual enzymatic method for simultaneous quantification of cholesterol and triglycerides in lipoproteins by HPLC. *J. Lipid Res.* **43**, 805–814
19. Bligh, E. G., and Dyer, W. J. (1959) A rapid method of total lipid extraction and purification. *Can. J. Biochem. Physiol.* **37**, 911–917
20. Bochud, M., Marquant, F., Marques-Vidal, P. M., Vollenweider, P., Beckmann, J. S., Mooser, V., Paccaud, F., and Rousson, V. (2009) Association between C-reactive protein and adiposity in women. *J. Clin. Endocrinol. Metab.* **94**, 3969–3977
21. Jung, U. J., and Choi, M. S. (2014) Obesity and its metabolic complications: the role of adipokines and the relationship between obesity, inflammation, insulin resistance, dyslipidemia and nonalcoholic fatty liver disease. *Int. J. Mol. Sci.* **15**, 6184–6223
22. Nijhuis, J., Rensen, S. S., Slaats, Y., van Dielen, F. M., Buurman, W. A., and Greve, J. W. (2009) Neutrophil activation in morbid obesity, chronic activation of acute inflammation. *Obesity (Silver Spring)* **17**, 2014–2018
23. Wang, J., Badeanlou, L., Bielawski, J., Ciaraldi, T. P., and Samad, F. (2014) Sphingosine kinase 1 regulates adipose proinflammatory responses and insulin resistance. *Am. J. Physiol. Endocrinol. Metab.* **306**, E756–E768

24. Chen, S., Okahara, F., Osaki, N., and Shimotoyodome, A. (2015) Increased GIP signaling induces adipose inflammation via a HIF-1α-dependent pathway and impairs insulin sensitivity in mice. *Am. J. Physiol. Endocrinol. Metab.* **308**, E414–E425
25. Joo, E., Harada, N., Yamane, S., Fukushima, T., Taura, D., Iwasaki, K., Sankoda, A., Shibue, K., Harada, T., Suzuki, K., Hamasaki, A., and Inagaki, N. (2017) Inhibition of gastric inhibitory polypeptide receptor signaling in adipose tissue reduces insulin resistance and hepatic steatosis in high-fat diet-fed mice. *Diabetes* **66**, 868–879
26. Lee, Y. S., Park, M. S., Choung, J. S., Kim, S. S., Oh, H. H., Choi, C. S., Ha, S. Y., Kang, Y., Kim, Y., and Jun, H. S. (2012) Glucagon-like peptide-1 inhibits adipose tissue macrophage infiltration and inflammation in an obese mouse model of diabetes. *Diabetologia* **55**, 2456–2468
27. Nasteska, D., Harada, N., Suzuki, K., Yamane, S., Hamasaki, A., Joo, E., Iwasaki, K., Shibue, K., Harada, T., and Inagaki, N. (2014) Chronic reduction of GIP secretion alleviates obesity and insulin resistance under high-fat diet conditions. *Diabetes* **63**, 2332–2343
28. Ballinger, A. (2003) Gastric inhibitory polypeptide links overnutrition to obesity. *Gut* **52**, 319–320
29. Yabe, D., and Seino, Y. (2011) Two incretin hormones GLP-1 and GIP: comparison of their actions in insulin secretion and β cell preservation. *Prog. Biophys. Mol. Biol.* **107**, 248–256
30. Pennington, K. L., and DeAngelis, M. M. (2016) Epidemiology of age-related macular degeneration (AMD): associations with cardiovascular disease phenotypes and lipid factors. *Eye Vis. (Lond.)* **3**, 34
31. Farr, S., Taher, J., and Adeli, K. (2014) Glucagon-like peptide-1 as a key regulator of lipid and lipoprotein metabolism in fasting and postprandial states. *Cardiovasc. Hematol. Disord. Drug Targets* **14**, 126–136
32. Wang, X. C., Gusdon, A. M., Liu, H., and Qu, S. (2014) Effects of glucagon-like peptide-1 receptor agonists on non-alcoholic fatty liver disease and inflammation. *World J. Gastroenterol.* **20**, 14821–14830
33. Marques, C., Mega, C., Gonçalves, A., Rodrigues-Santos, P., Teixeira-Lemos, E., Teixeira, F., Fontes-Ribeiro, C., Reis, F., and Fernandes, R. (2014) Sitagliptin prevents inflammation and apoptotic cell death in the kidney of type 2 diabetic animals. *Mediators Inflamm.* **2014**, 538737
34. Iwai, T., Ito, S., Tanimitsu, K., Udagawa, S., and Oka, J. (2006) Glucagon-like peptide-1 inhibits LPS-induced IL-1beta production in cultured rat astrocytes. *Neurosci. Res.* **55**, 352–360
35. Dobrian, A. D., Ma, Q., Lindsay, J. W., Leone, K. A., Ma, K., Coben, J., Galkina, E. V., and Nadler, J. L. (2011) Dipeptidyl peptidase IV inhibitor sitagliptin reduces local inflammation in adipose tissue and in pancreatic islets of obese mice. *Am. J. Physiol. Endocrinol. Metab.* **300**, E410–E421
36. Schirra, J., Sturm, K., Leicht, P., Arnold, R., Göke, B., and Katschinski, M. (1998) Exendin(9-39)amide is an antagonist of glucagon-like peptide-1(7-36)amide in humans. *J. Clin. Invest.* **101**, 1421–1430
37. Kadowaki, T., Yamauchi, T., Kubota, N., Hara, K., Ueki, K., and Tobe, K. (2006) Adiponectin and adiponectin receptors in insulin resistance, diabetes, and the metabolic syndrome. *J. Clin. Invest.* **116**, 1784–1792
38. Engeli, S., Feldpausch, M., Gorzelniak, K., Hartwig, F., Heintze, U., Janke, J., Möhlig, M., Pfeiffer, A. F., Luft, F. C., and Sharma, A. M. (2003) Association between adiponectin and mediators of inflammation in obese women. *Diabetes* **52**, 942–947
39. Choi, K. M., Ryu, O. H., Lee, K. W., Kim, H. Y., Seo, J. A., Kim, S. G., Kim, N. H., Choi, D. S., and Baik, S. H. (2007) Serum adiponectin, interleukin-10 levels and inflammatory markers in the metabolic syndrome. *Diabetes Res. Clin. Pract.* **75**, 235–240
40. Kim, J. Y., van de Wall, E., Laplante, M., Azzara, A., Trujillo, M. E., Hofmann, S. M., Schraw, T., Durand, J. L., Li, H., Li, G., Jelicks, L. A., Mehler, M. F., Hui, D. Y., Deshaies, Y., Shulman, G. I., Schwartz, G. J., and Scherer, P. E. (2007) Obesity-associated improvements in metabolic profile through expansion of adipose tissue. *J. Clin. Invest.* **117**, 2621–2637
41. Hotta, K., Funahashi, T., Arita, Y., Takahashi, M., Matsuda, M., Okamoto, Y., Iwahashi, H., Kuriyama, H., Ouchi, N., Maeda, K., Nishida, M., Kihara, S., Sakai, N., Nakajima, T., Hasegawa, K., Muraguchi, M., Ohmoto, Y., Nakamura, T., Yamashita, S., Hanafusa, T., and Matsuzawa, Y. (2000) Plasma concentrations of a novel, adipose-specific protein, adiponectin, in type 2 diabetic patients. *Arterioscler. Thromb. Vasc. Biol.* **20**, 1595–1599
42. Ouchi, N., Kihara, S., Funahashi, T., Matsuzawa, Y., and Walsh, K. (2003) Obesity, adiponectin and vascular inflammatory disease. *Curr. Opin. Lipidol.* **14**, 561–566
43. Ryo, M., Nakamura, T., Kihara, S., Kumada, M., Shibazaki, S., Takahashi, M., Nagai, M., Matsuzawa, Y., and Funahashi, T. (2004) Adiponectin as a biomarker of the metabolic syndrome. *Circ. J.* **68**, 975–981
44. Shetty, G. K., Economides, P. A., Horton, E. S., Mantzoros, C. S., and Veves, A. (2004) Circulating adiponectin and resistin levels in relation to metabolic factors, inflammatory markers, and vascular reactivity in diabetic patients and subjects at risk for diabetes. *Diabetes Care* **27**, 2450–2457
45. Côté, M., Mauriège, P., Bergeron, J., Alméras, N., Tremblay, A., Lemieux, I., and Després, J. P. (2005) Adiponectinemia in visceral obesity: impact on glucose tolerance and plasma lipoprotein and lipid levels in men. *J. Clin. Endocrinol. Metab.* **90**, 1434–1439
46. Yamauchi, T., and Kadowaki, T. (2008) Physiological and pathophysiological roles of adiponectin and adiponectin receptors in the integrated regulation of metabolic and cardiovascular diseases. *Int. J. Obes.* **32** (Suppl 7), S13–S18
47. Maceyka, M., Harikumar, K. B., Milstien, S., and Spiegel, S. (2012) Sphingosine-1-phosphate signaling and its role in disease. *Trends Cell Biol.* **22**, 50–60
48. Taha, T. A., Hannun, Y. A., and Obeid, L. M. (2006) Sphingosine kinase: biochemical and cellular regulation and role in disease. *J. Biochem. Mol. Biol.* **39**, 113–131
49. Qi, Y., Chen, J., Lay, A., Don, A., Vadas, M., and Xia, P. (2013) Loss of sphingosine kinase 1 predisposes to the onset of diabetes via promoting pancreatic β-cell death in diet-induced obese mice. *FASEB J.* **27**, 4294–4304

Received for publication August 24, 2018.
Accepted for publication January 22, 2019.

Supplemental Figures

Sphingosine kinase 1-interacting protein is a dual regulator of insulin and incretin secretion

Yanyan Liu[1], Shin-ichi Harashima[1], Yu Wang[1], Kazuyo Suzuki[1], Shinsuke Tokumoto[1], Ryota Usui[1], Hisato Tatsuoka[1], Daisuke Tanaka[1], Daisuke Yabe[1], Norio Harada[1], Yoshitaka Hayashi[2] and Nobuya Inagaki[1*]

Supplemental Figure 1. SKIP expression in adipose tissues.

Western blot of SKIP expression in perirenal, epididymal, mesenteric, brown, subcutaneous adipose tissues and islets from WT mice (n = 3).

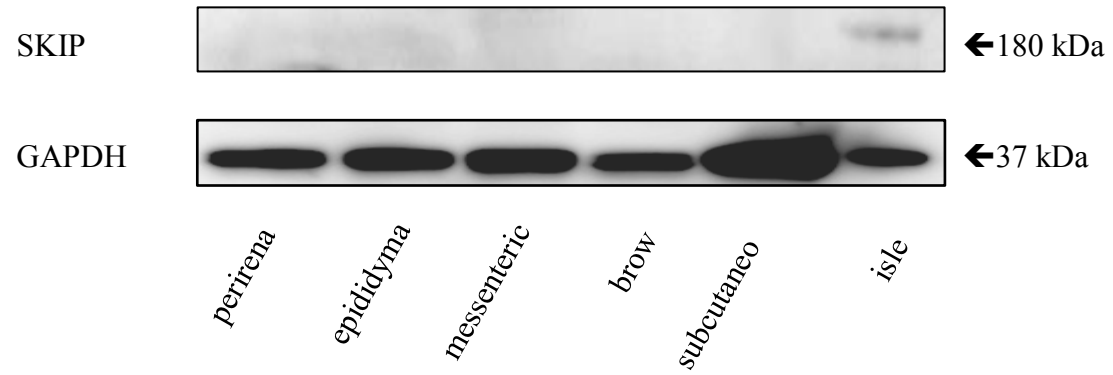

Supplemental Figure 2. Changes of blood glucose, insulin, total GIP and total GLP-1 in WT and SKIP$^{-/-}$ mice during OGTT. WT mice are represented by white bars and squares. SKIP$^{-/-}$ mice are represented by black bars and triangles. Changes of blood glucose (Δblood glucose) (A), insulin (Δinsulin) (B), total GIP (Δtotal GIP) (C) and total GLP-1 (Δtotal GLP-1) (D) as well as their incremental areas under the **curve** (iAUC) during OGTT. (A-D, n = 8). Values are mean ± SEM. In all panels, data were analyzed by ANOVA with Bonferroni's multiple comparisons test. *P < 0.05 and **P < 0.01 vs. WT female mice.

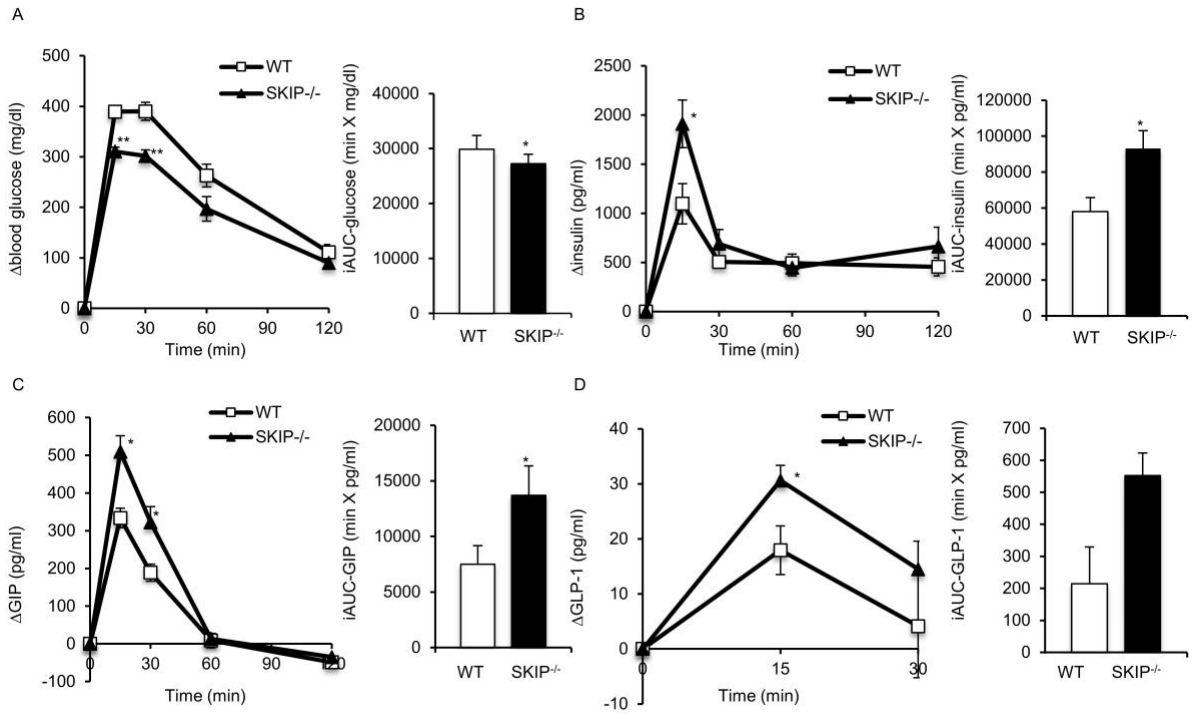

Supplemental Figure 3. SKIP-deficient female mice show improved glucose tolerance by increased insulin and GIP secretions. WT female mice are represented by white bars and squares. SKIP$^{-/-}$ female mice are represented by black bars and triangles. (A) Body weight change in WT and SKIP$^{-/-}$ female mice. Absolute values of blood glucose (B), insulin (D), and total GIP (F) in WT and SKIP$^{-/-}$ female mice. Changes of blood glucose (Δblood glucose) (C), insulin (Δinsulin) (E) and total GIP (Δtotal GIP) (G) as well as their incremental areas under the curve (iAUC) during OGTT in WT and SKIP$^{-/-}$ female mice. (A-D, n = 4). Values are mean ± SEM. Panels A-D were analyzed by 2-way ANOVA with Bonferroni post-hoc test or Student' s *t* test. *P < 0.05, **P < 0.01 vs. WT mice.

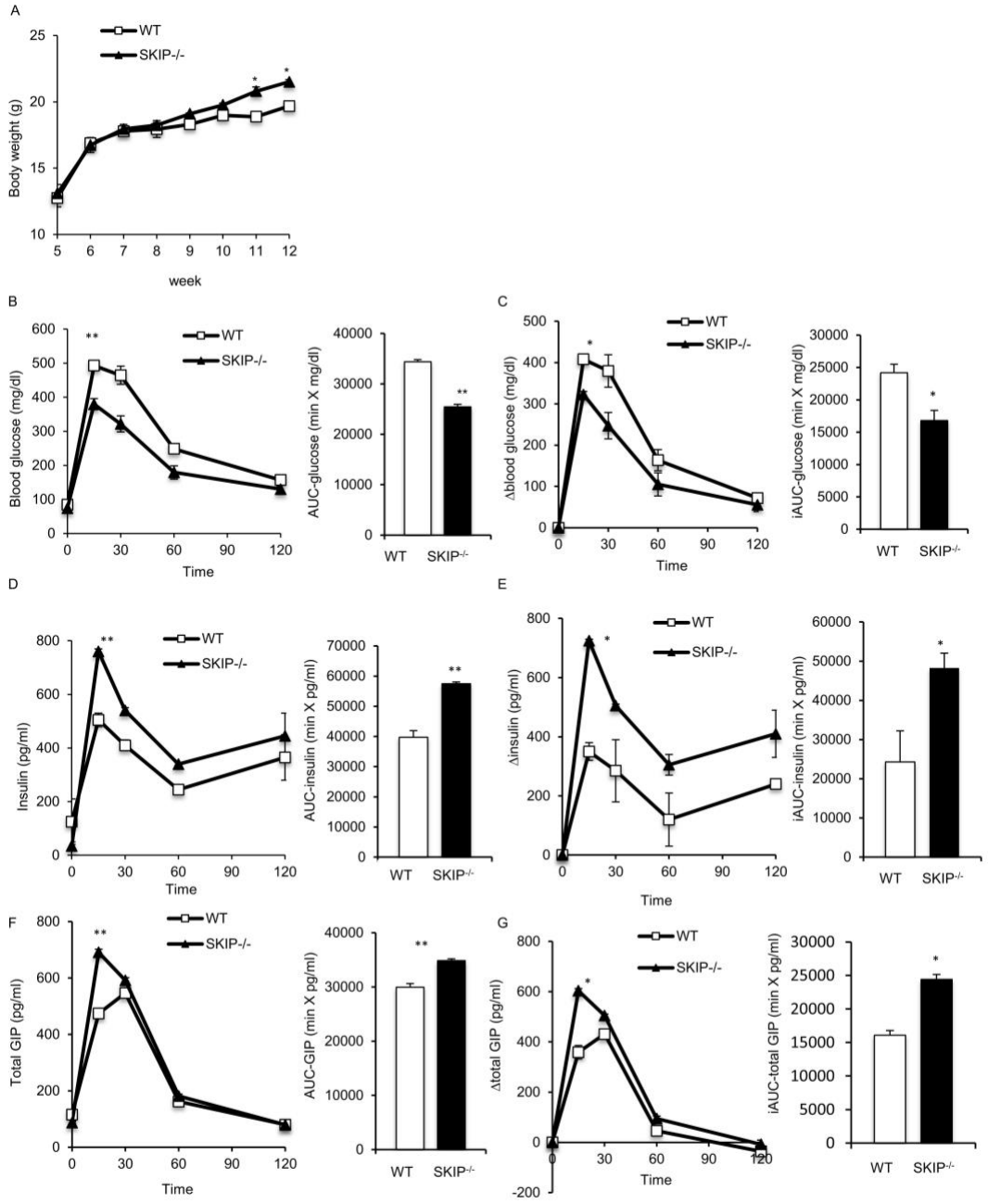

Supplemental Figure 4. Triglyceride and cholesterol synthesis enzyme levels in WT and SKIP$^{-/-}$ mice. (A) Gene expression involved in triglyceride synthesis. (B) Gene expression involved in total cholesterol synthesis between WT and SKIP$^{-/-}$ mice (A, B, n = 4). Values are mean ± SEM. In all panels, data were analyzed by student's *t* test. *P < 0.05, **P < 0.01vs. WT mice. SREBP-1c, sterol regulatory element-binding protein -1c; ACS, acetyl-CoA synthetase; ACC, acetyl-CoA carboxylase; FAS, fatty acid synthase; SCD1, stearoyl-CoA desaturaseadenosine 1; ACL, ATP citrate lyase; HMGS, hydroxymethylglutaryl-CoA synthase; HMGR, hydroxymethylglutaryl-CoA reductase; FPPS, farnesyl pyrophosphate synthase; and RPS18, ribosomal protein S18.

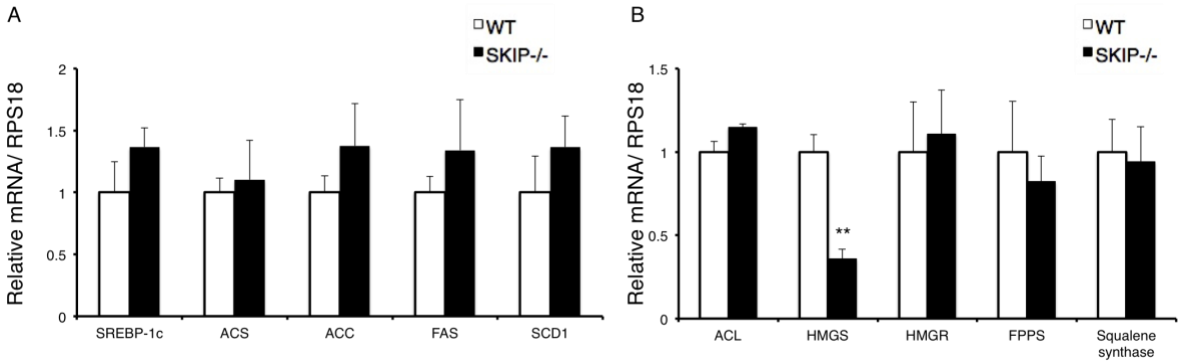

Supplemental Figure 5. Sphingosine kinase 1 expression and sphingosine kinase activity in WT and SKIP$^{-/-}$ mice. (A) Quantitative real-time PCR analysis of sphingosine kinase-1 mRNA in liver and adipose tissues from WT and SKIP$^{-/-}$ mice. (B) Serum sphingosine kinase activity in both WT and SKIP$^{-/-}$ mice. (A and B, n = 4). Values are mean ± SEM. In all panels, data were analyzed by Student's *t* test. *P < 0.05, **P < 0.01 vs. WT mice. RLU, relative light unit; RPS18, ribosomal protein S18; and SPHK, sphingosine kinase.

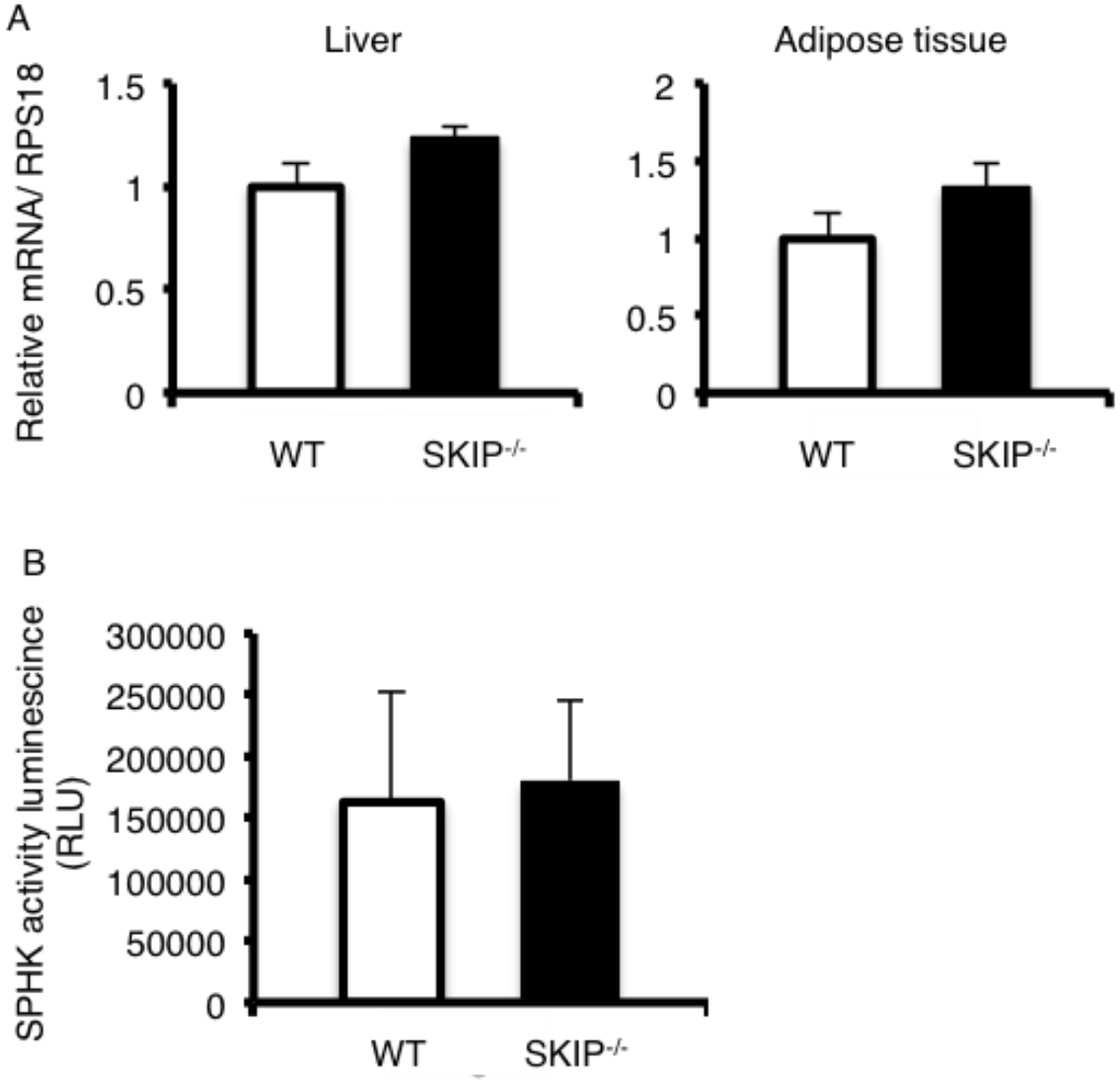

Supplemental Figure 6. Changes of blood glucose, insulin, total GIP and total GLP-1 in WT, SKIP$^{-/-}$, GIP$^{gfp/gfp}$, and SKIP$^{-/-}$GIP$^{gfp/gfp}$ mice during OGTT. WT mice are represented by white bars and squares, SKIP$^{-/-}$ mice are represented by black bars and squares, GIP$^{gfp/gfp}$ mice are represented by blue bars and squares, SKIP$^{-/-}$GIP$^{gfp/gfp}$ mice are represented by red bars and squares. Changes of blood glucose (Δblood glucose) (A), insulin (Δinsulin) (B), total GIP (Δtotal GIP) (C) and total GLP-1 (Δtotal GLP-1) (D) as well as their incremental areas under the curve (iAUC) during OGTT. (A-D, n = 8). Values are mean ± SEM. In all panels, data were analyzed by ANOVA with Bonferroni's multiple comparisons test. *P < 0.05 and **P < 0.01 vs. WT mice; § P < 0.05 and §§ P < 0.01 vs. SKIP$^{-/-}$ mice; ¶ P < 0.05 and ¶¶ P < 0.01 vs. GIP$^{gfp/gfp}$ mice.

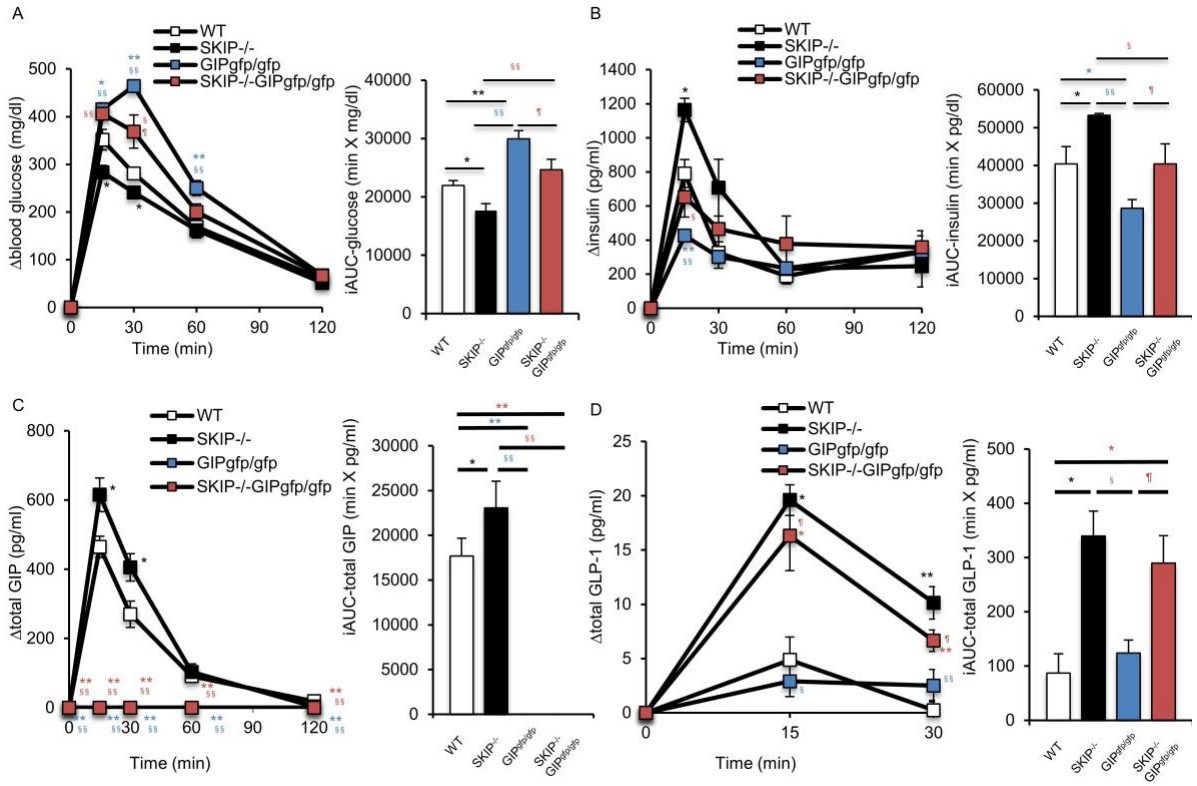

Supplemental Figure 7. Changes of blood glucose, insulin, total GIP and total GLP-1 in WT and SKIP$^{-/-}$ mice treated with or without Exendin (9-39) during oral glucose tolerance test (OGTT). Vehicle- treated WT mice are represented by white bars and squares. Vehicle- treated SKIP$^{-/-}$ mice are represented by black bars and squares. Exendin (9-39)- [Ex-(9-39)]-treated WT mice are represented by blue bars and blue squares. Exendin (9-39) [Ex-(9-39)]-treated SKIP$^{-/-}$ mice are represented by red bars and squares. Changes of blood glucose (Δblood glucose) (A), insulin (Δinsulin) (B), total GIP (Δtotal GIP) (C) and total GLP-1 (Δtotal GLP-1) (D) as well as their incremental areas under the curve (iAUC) during OGTT. (A-B, n = 6). Values are mean ± SEM. In all panels, data were analyzed by ANOVA with Bonferroni's multiple comparisons test. *P < 0.05 and **P < 0.01 vs. WT mice; § P < 0.05 and § § P < 0.01 vs. SKIP$^{-/-}$ mice; ¶ P < 0.05 and ¶¶ P < 0.01 vs. WT-Ex (9-39)-treated mice.

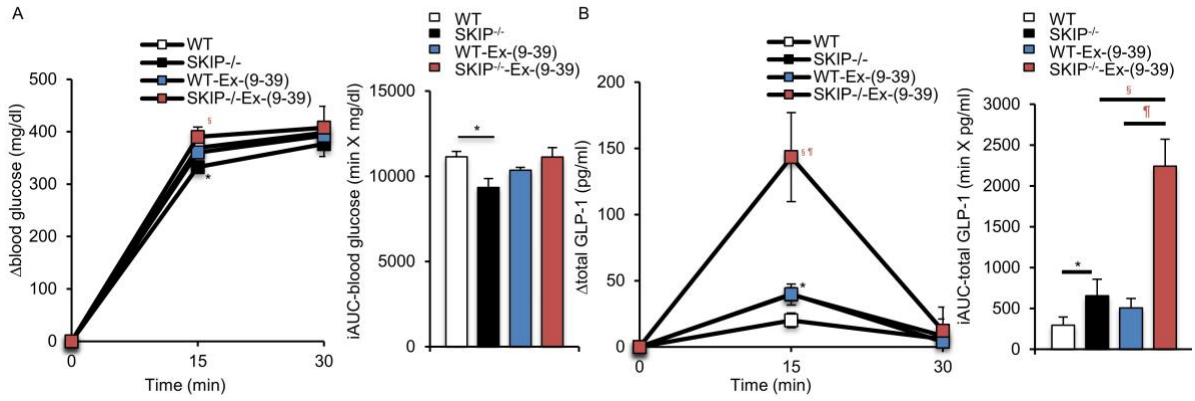

Supplemental Tables

Sphingosine kinase 1-interacting protein is a dual regulator of insulin and incretin secretion

Yanyan Liu[1], Shin-ichi Harashima[1], Yu Wang[1], Kazuyo Suzuki[1], Shinsuke Tokumoto[1], Ryota Usui[1], Hisato Tatsuoka[1], Daisuke Tanaka[1], Daisuke Yabe[1], Norio Harada[1], Yoshitaka Hayashi[2] and Nobuya Inagaki[1*]

Supplemental Table 1. List of gene primers (5′ to 3′)

Target genes	Forward primer	Reverse primer
SKIP	ACC ATG GAT GTC AAC TCC CGG CTT	GTT TTC TGA CTC ATC TTC CAC AAA C
IL-1β	GCA ACT GTT CCT GAA CTC AAC T	ATC TTT TGG GGT CCG TCA ACT
IL-6	CCA CTT CAC AAG TCG GAG GCT TA	CCA GTT TGG TAG CAT CCA TCA TTT C
TNF-α	GAG AAA GTC AAC CTC CTC TCT G	GAA GAC TCC TCC CAG GTA TAT G
IL-10	AAG GAC CAG CTG GAC AAC AT	TTT TCA CAG GGG AGA AAT CG
Adiponectin	GGA ACT TGT GCA GGT TGG AT	GCT TCT CCA GGC TCT CCT TT
F4/80	TGC GGG ATT CCT ACA CTA TCT T	CGT CTC TGT ATT CAA CCA GCA G
MCP-1	AGC AGC AGG TGT CCC AAA GA	GTG CTG AAG ACC TTA GGG CAG A
ICAM	AAC TGT GGC ACC GTG CAG TC	AGG GTG AGG TCC TTG CCT ACT TG
VCAM	TTC CGG CAT TTA TGT GTG TGA AG	GGCACATTTCCACAAGTGCAG

Supplemental Table 2. Microarray analysis of SKIP expression in GFP positive cells and negative cells from $GIP^{gfp/+}$ and $Gcg^{gfp/+}$ mice.

SKIP Expression	GFP-Positive	GFP-Negative	Ratio	*P*
$GIP^{gfp/+}$	377.6	23.87	15.82	0.008
$Gcg^{gfp/+}$	92.63	26.6	3.48	0.031

All data are expressed as the mean ± SEM (n = 8), data were analyzed by Student's *t* test. A significant difference was considered at $p < 0.05$.